Fault interaction and stress triggering

Types of interactions

Interaction type	*Perturbation effects*	*Spatial scale*	*Temporal scale*
Dynamic	- Rupture propagation; - Arrest	1 – 60 Km	1 – 20 s
Static	- Earthquake triggering; - Off – faults aftershocks; - Sesimicity rate change	1 – 60 Km 1 – 60 Km 1 – 100 Km	minutes – few years
Post – seismic	Long – term stress changes	10 – 1000 Km	few years – centuries

Coulomb Failure Function

Following the Coulomb' s failure assumption we define a Coulomb Failure Stress as (e. g. *Jaeger and Cook,1969*):

$$CFS = \|\mathrm{T}\| + \mu\left(\sigma_n + p_{fluid}\right) - C$$

where: $\|\mathrm{T}\|$ is the shear tration modulus,

μ is the coefficient of friction,

σ_n is the normal stress (positive in tension),

p_{fluid} is the pore fluid pressure,

C is the cohesion.

Assuming μ and C constant over time, we have the Coulomb Failure Stress change:

$$\Delta CFS = \Delta\|\mathrm{T}\| + \mu\left(\Delta\sigma_n + \Delta p_{fluid}\right)$$

where it has been assumed an isotropic failure plane.

ΔCFS is used to evaluate if one earthquake brought another earthquake closer to, or farther from, failure:

$\Delta CFS > 0 \Rightarrow$ fault plane loaded $\Rightarrow$ closer to failure

$\Delta CFS < 0 \Rightarrow$ fault plane relaxed $\Rightarrow$ farther from failure

(Stress Shadow)

Neglecting the spatial dependence in tractions, are:

$$\mathrm{T}(t) = \mathrm{T}(0) + \Delta\mathrm{T}(t) \qquad \sigma_n(t) = \sigma_n(0) + \Delta\sigma_n(t) \qquad p_{fluid}(t) = p_{fluid}(0) + \Delta p_{fluid}(t)$$

Therefore we can write:

$$\Delta CFS(t) = \|\,\mathrm{T}(0) + \Delta\mathrm{T}(t)\,\| - \|\,\mathrm{T}(0)\,\| + \mu\left(\Delta\sigma_n(t) + \Delta p_{fluid}(t)\right)$$

$\Delta\|\mathrm{T}\|$ is the change in shear stress due to the first earthquake and it is resolved in the slip direction of the second earthquake;

$\Delta\sigma_n$ is the change in normal stress due to the first earthquake and it is resolved in the direction orthogonal to the fault plane of the second earthquake.

Stress changes approaches (after *Harris, 1998*)

Method	Parameters Required	Successes	Problems	Authors
Static Coulomb failure stress (elastic) ΔCFS	mainshock static slip model, μ', and $\Delta\sigma$, $\Delta\tau$, $\dot{\tau}$, on known fault planes and known slip directions*	ΔCFS > 0 explains locations of aftershocks that do occur, ΔCFS < 0 predicts shadows (timing and locations); may give rupture extent	many ΔCFS > 0 faults do not experience subsequent large earthquakes, so it is hard to use ΔCFS > 0 as a predictive tool	*Smith and Van de Lindt* [1969], *Rybicki* [1973], *Yamashina* [1978], *Stein and Lisowski* [1983], *Simpson et al.* [1988], *Yoshioka and Hashimoto* [1989a, b], *Reasenberg and Simpson* [1992], etc. (see text for more authors); *Crider and Pollard* [this issue], *Hardebeck et al.* [this issue], *Harris and Simpson* [this issue], *Kagan and Jackson* [this issue], *Nalbant et al.* [this issue], *Nostro et al.* [this issue], *Taylor et al.* [this issue], and *Toda et al.* [this issue]
Dynamic Coulomb failure stress (elastic) ΔCFS(t)	mainshock dynamic fault slip model, μ', and $\Delta\sigma(t)$, $\Delta\tau(t)$ on known fault planes and known slip directions*	may predict rupture lengths, given fault geometry	does not explain long delays (more than tens of seconds) between subevents; needs more testing	*Harris et al.* [1991], *Harris and Day* [1993], *Hill et al.* [1993], *Gomberg and Bodin* [1994], *Spudich et al.* [1994, 1995], *Cotton and Coutant* [1997], etc.
Static rate and state	mainshock static slip model, $\Delta\sigma$, $\Delta\tau$, σ, τ, $\dot{\tau}$, A, B, D_c, H, time of last event, recurrence interval (to determine slip speed)	seems to predict aftershock duration	needs more testing; rate-and-state parameters defined in the laboratory, but not known for the Earth	*Dieterich* [1994], *Dieterich and Kilgore* [1996], *Roy and Marone* [1996], *Gross and Bürgmann* [1998], *Gomberg et al.* [this issue], *Harris and Simpson* [this issue], and *Toda et al.* [this issue]
Dynamic rate and state	mainshock dynamic fault slip model, $\Delta\sigma(t)$, $\Delta\tau(t)$, σ, τ, $\dot{\tau}$, A, H, time of last event, slip speed	may explain remote triggering	needs more testing; still need to define rate-and-state parameters in the Earth; inertial terms not yet included in models	*Dieterich* [1987] and *Gomberg et al.* [1997, this issue]
Static Coulomb failure stress (viscoelastic)	mainshock slip model, Maxwell relaxation time, relaxing layer thickness	may explain time delays between mainshock and subsequent events, also irregular recurrence intervals	needs more testing, also needs more geodetic data to confirm viscoelastic parameters	*Dmowska et al.* [1988], *Roth* [1988], *Ghosh et al.* [1992], *Ben-Zion et al.* [1993], *Taylor et al.* [1996], *Pollitz and Sacks* [1997], *Freed and Lin* [this issue]
Fluid flow	mainshock slip model, permeability tensor	may explain time delays between mainshock and subsequent events	may not be successful at predicting both the spatial and temporal aftershock pattern	*Li et al.* [1987], *Hudnut et al.* [1989], *Noir et al.* [1997], etc.; *Seeber et al.* [this issue]

*If the aftershock fault planes are not known, then some authors assume optimally oriented faults; this requires knowledge of the background stress directions.

1 – D Spring – slider model

Numerical Method: RK SS

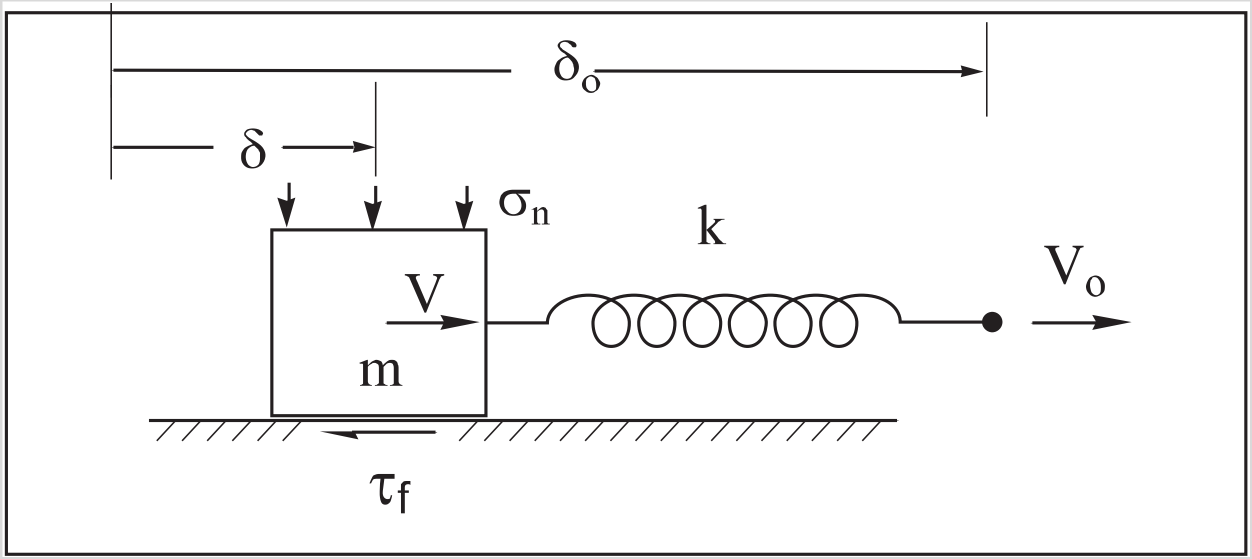

$$m\,\ddot{\delta} = k\,(\delta_o - \delta) - \tau_f + \Delta\tau, \quad \Delta\tau(t) \text{ perturbazione}$$

τ_f = resistenza di attrito

Reologia: **attrito rate- and state-dependent**

θ (Φ) = variabile di stato della superficie, $V = \dot{\delta}$ velocità

A - Ruina-Dieterich	**B - Dieterich - Ruina**
$\tau_f = \tau_* + \theta + A \ln \left(\frac{V}{V_*}\right)$	$\tau_f = \tau_* - A \ln \left(\frac{V_*}{V}\right) + B \ln \left(\frac{\Phi V_*}{L}\right)$
$\frac{d\theta}{dt} = -\frac{V}{L}\,\theta + B \ln \frac{V}{V_*}$	$\frac{d\Phi}{dt} = 1 - \frac{\Phi V}{L}$

Stato del sistema: **(V(t), d (t), t_f(t))**

o condizioni mecc. faglia

appross. q. statica **(V (t), t_f(t))**

$V<V_C$=0.1 mm/s

Inertia is negligible and the system passes through a sequence of equilibrium states

Fault seismic cycle modeling

1-D

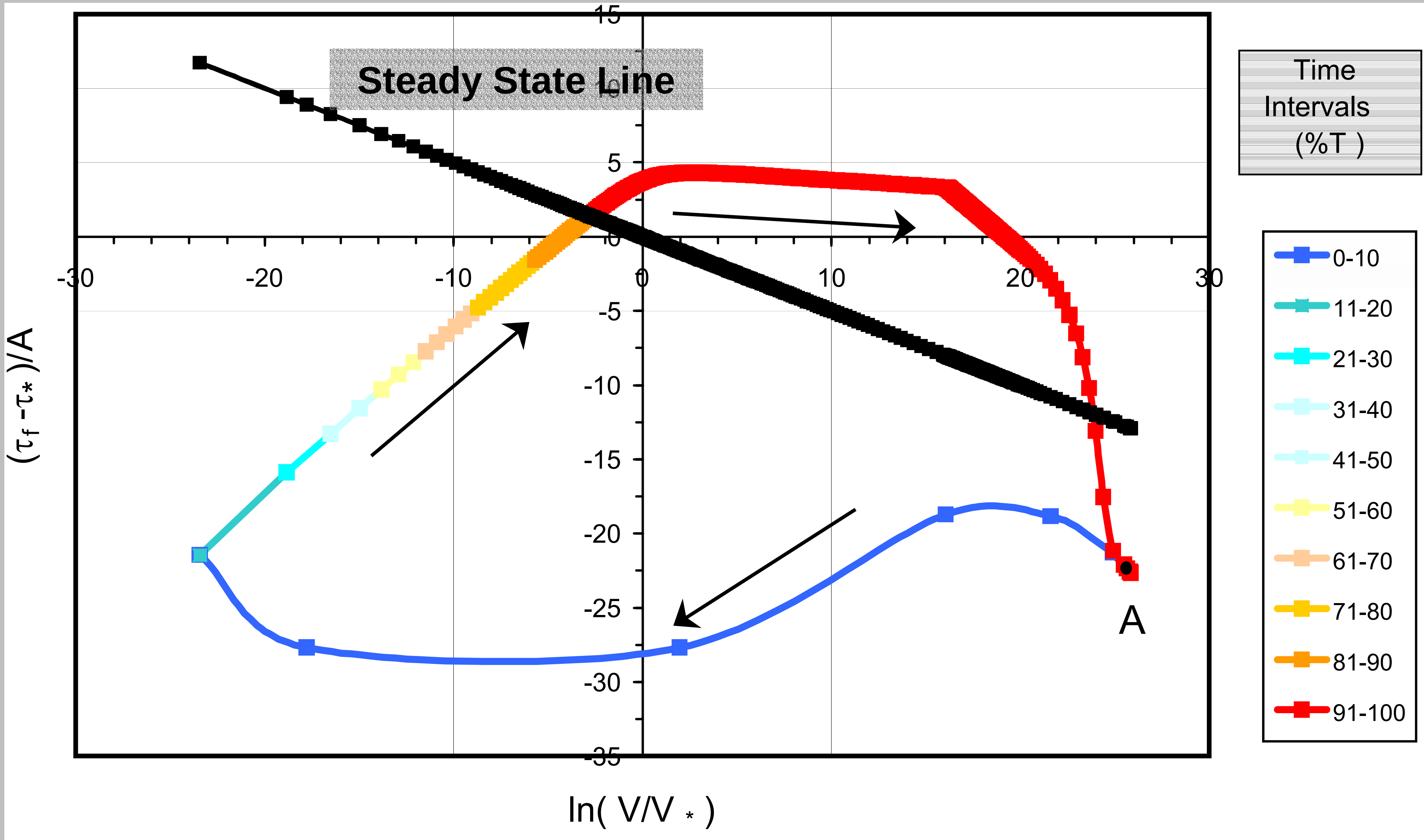

Analytical stress perturbations

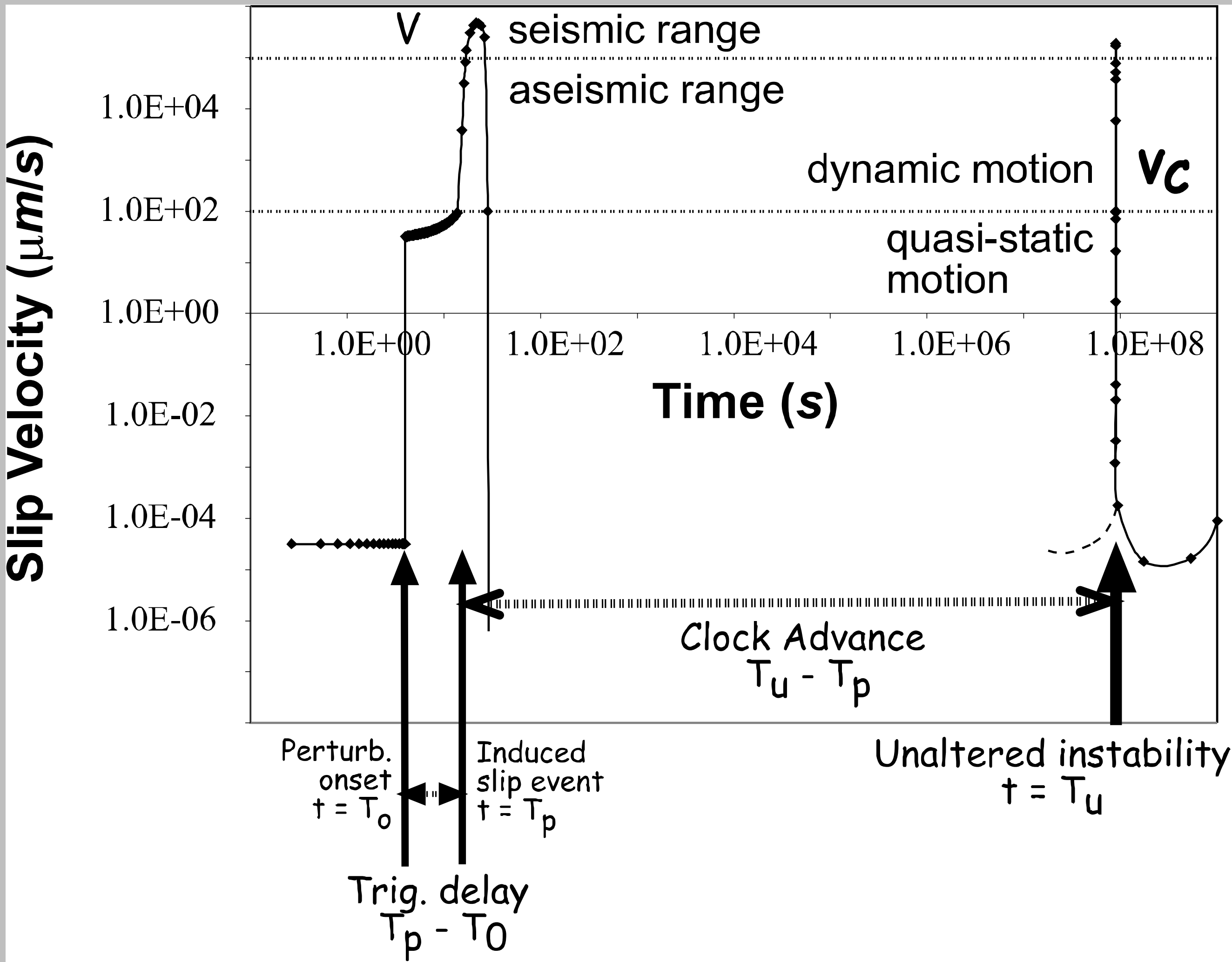

Analytical stress perturbations
The step and the pulse #1

Step

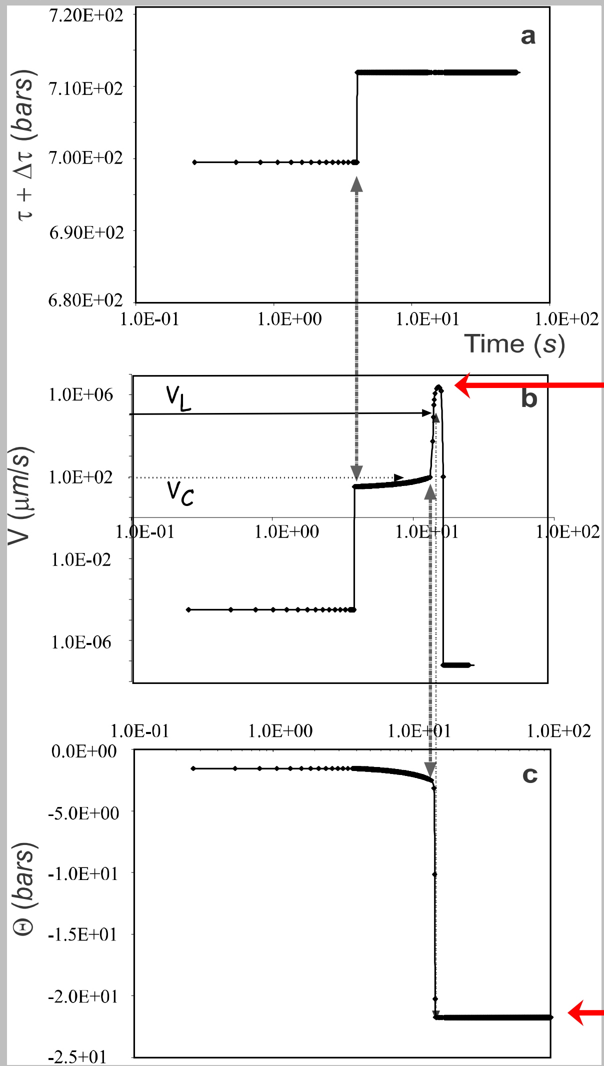

Pulse

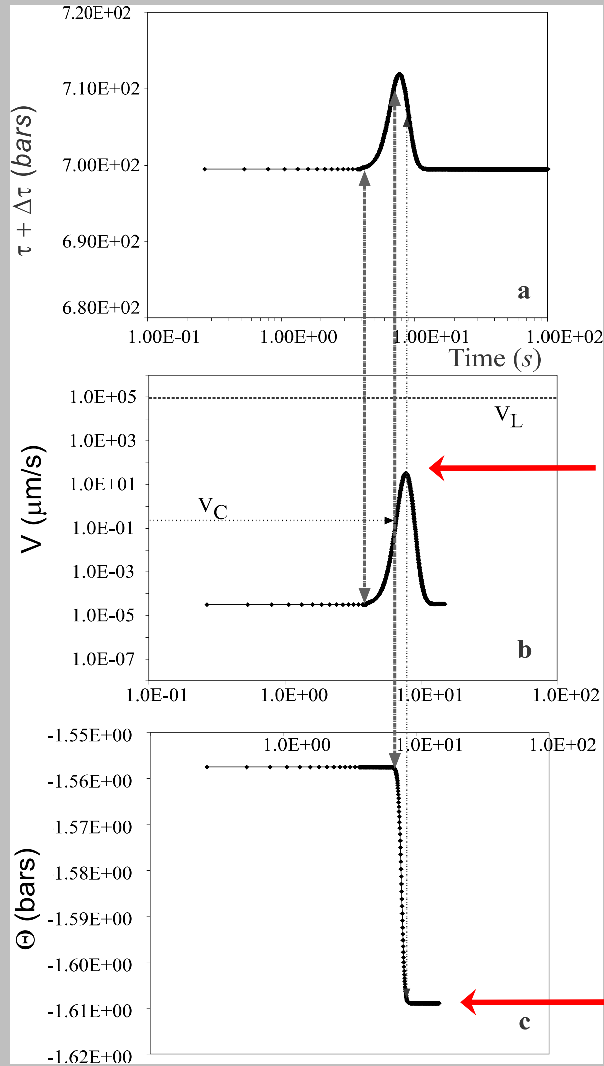

Analytical stress perturbations
The step and the pulse #2

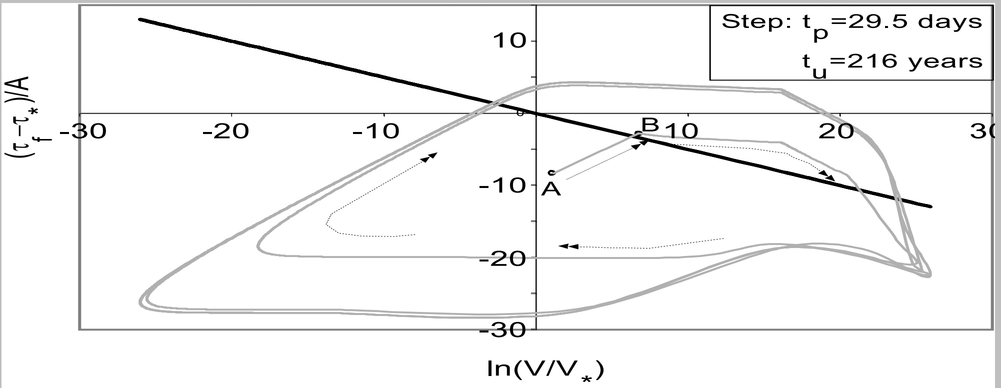

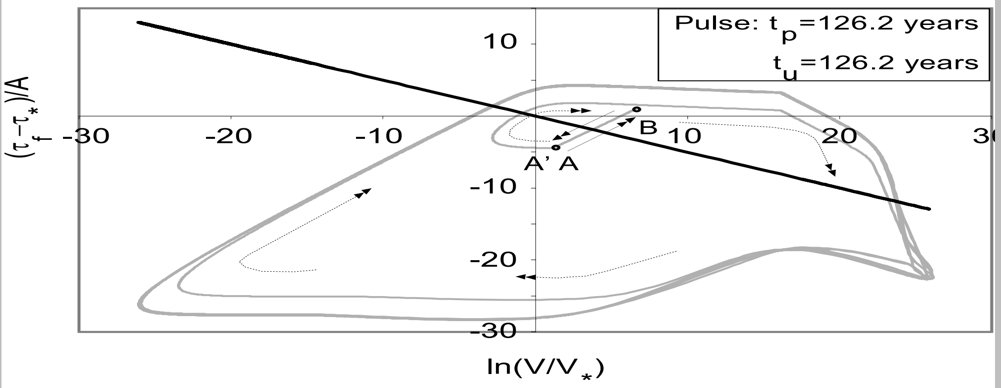

Realistic stress perturbations
Syntetic seismograms #1

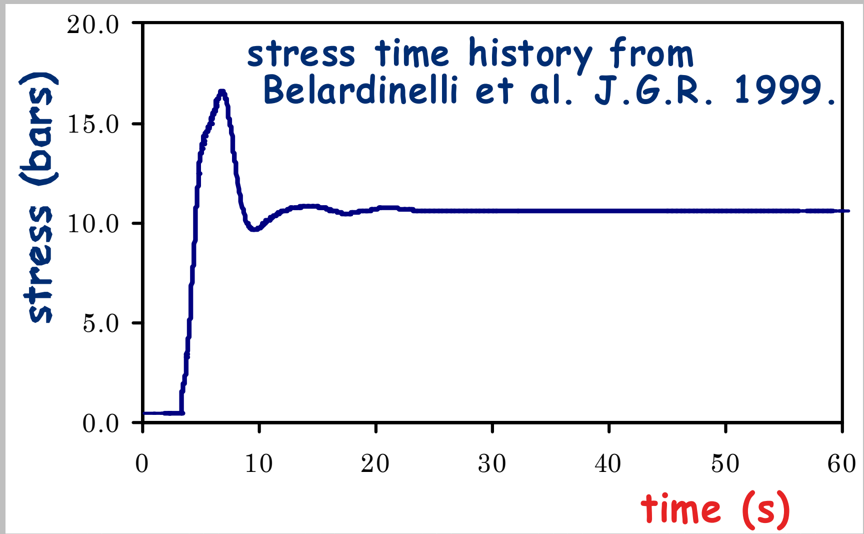

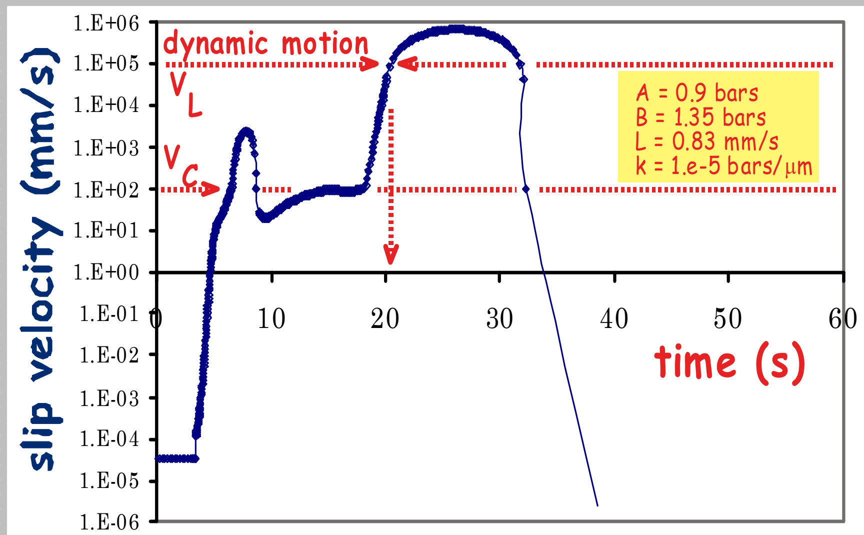

Realistic stress perturbations
Syntetic seismograms #2

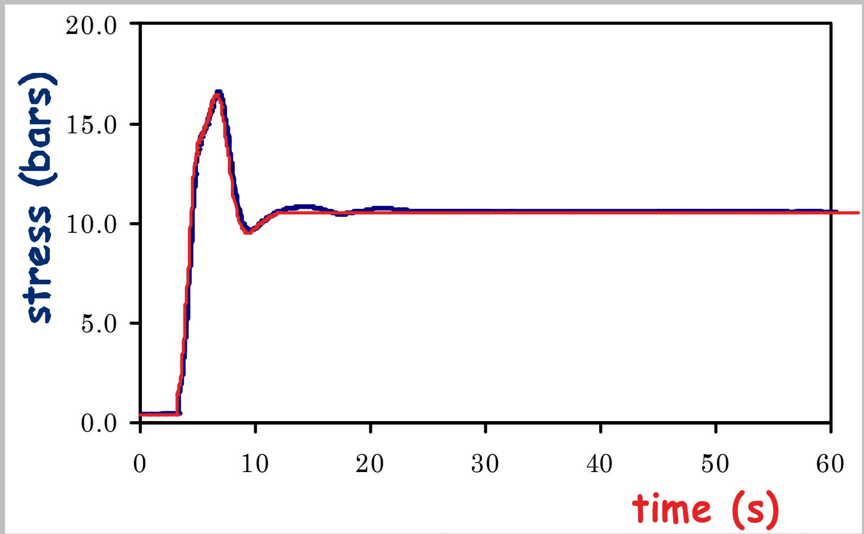

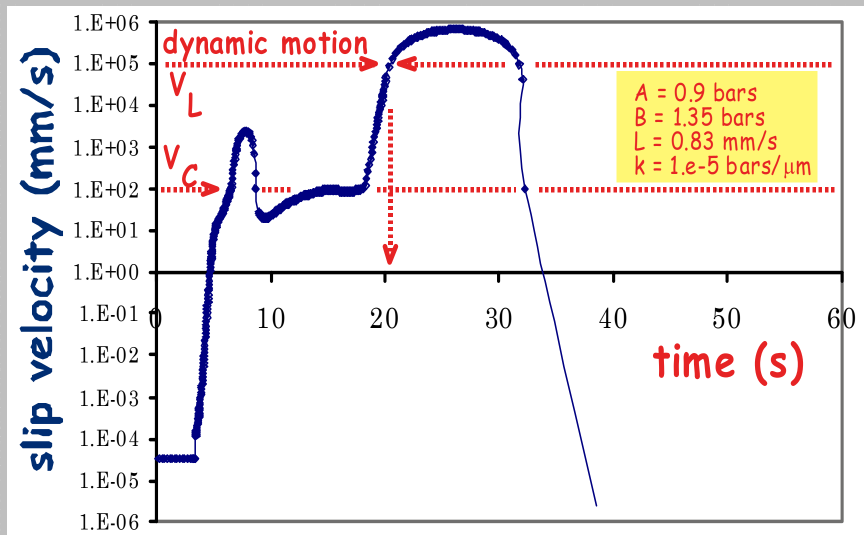


Fault interaction by
dynamic stress transfer:
the case of the 2000 South
Iceland seismic sequence
Part I

Motivations and Goals

- To evidence the eventual effect of the transient part of the coseismic stress changes due to the 17 June 2000, M 6.6 South Iceland earthquake;
- The debate on the triggering potential of transient stress changes is still open;
- The observational evidences are difficult and few.

The choice of the events

- The largest events (M ~ 5) occurring in the first five minutes
  - 8s, 26s, 30s, 130s, 226s
- in intermediate - far field
  - ~~8s~~, 26s, 30s, ~~130s~~, 226s
- that reasonably are not secondary aftershocks
  - 26s, 30s, ~~226s~~.

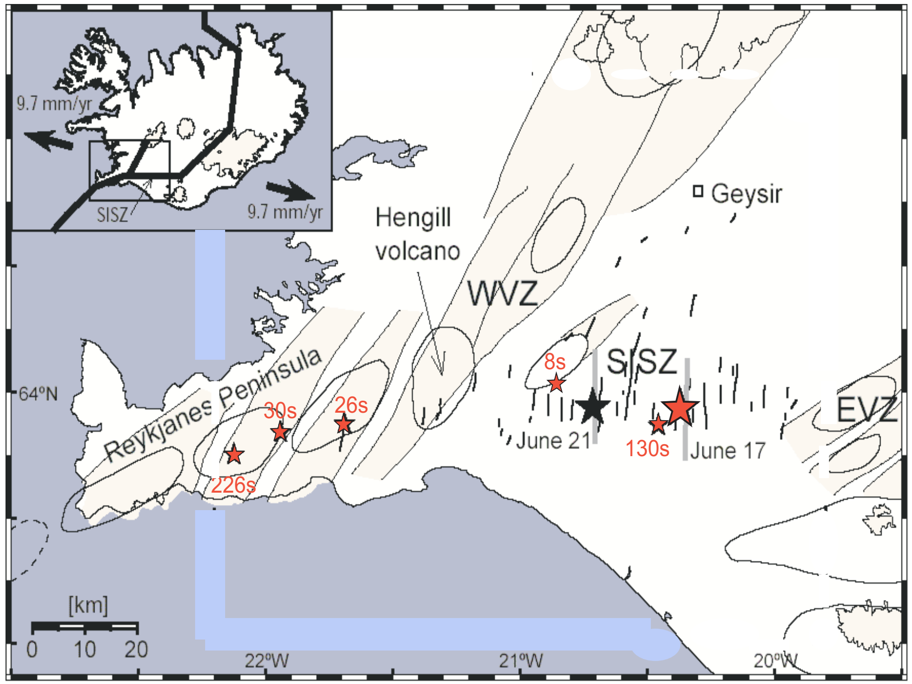

The 26 s and 30 s events

- They were not detected teleseismically.

- 26 s (64 km far)
  - –Not detected by DInSAR.
  - –Known fault.
- 30 s (77 km far)
  - – Waveforms partially obscured by the first event (mechanism uncertain)
  - – Detected by DInSAR and surface effects.
  - – August 2003: M 5 event on N-S fault with the same epicenter.

From SIL seismograms the 26 s and 30 s events occurred at the arrival (later than the first) of shear waves traveling at 2.5 km/s at their location.

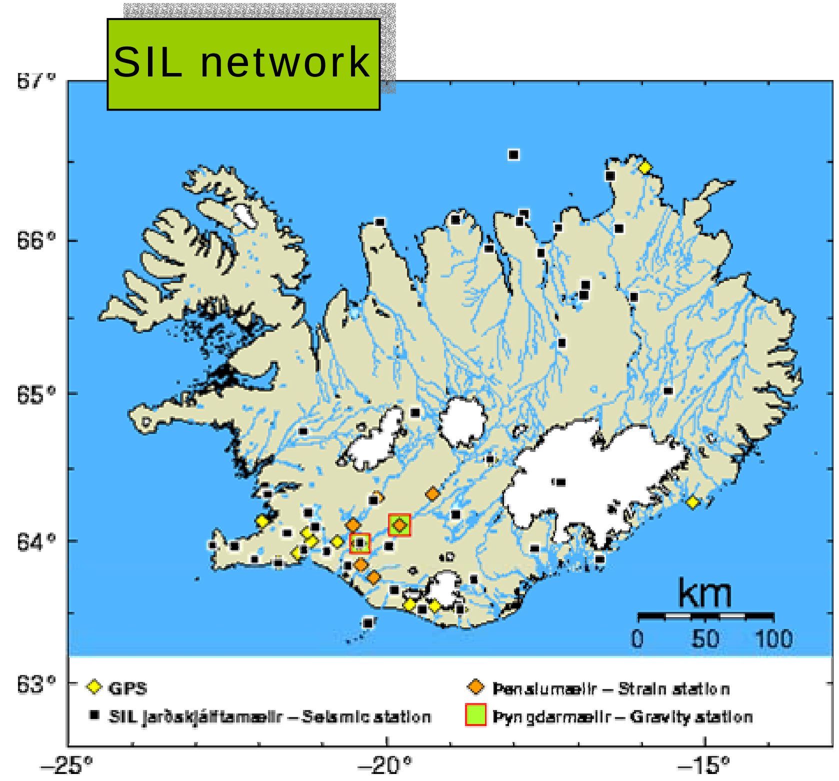

Event	Origin time	Latitude (°)	Longitude (°)	Depth (km)	M_L	M_{Lw}
26s	154106.9	63.951 ±0.004	-21.689 ±0.008	8.9 ±1.3	4.91	6
30s	154111.254	63.937 ±0.003	-21.94 ±0.01	3.8 ±1.3	4.68	5.9

Parameters used to compute the dynamic stress

- Slip distribution from geodetic data (Arnadottir et al. 2003). Right lateral strike slip fault, strike 7° E, dip 86°.
- Rupture history: bilateral Haskell model, rise time: 1-2 s, rupture velocity: 2.5 km /s.
- 2 crustal models with 4 layers:

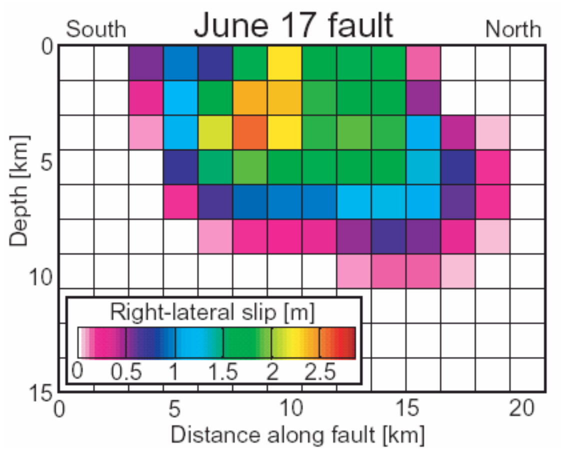

West of Hengill

Depth (km)	V_P (km/s)	V_S (km/s)	Density (kg/m^3)
0-3.1	3.3	1.85	2300
3.1-7.8	6.0	3.37	2900
7.8-17	6.85	3.88	3100
>17	7.5	4.21	3300

East of Hengill

Depth (km)	V_P (km/s)	V_S (km/s)	Density (kg/m^3)
0-1.1	3.2	1.81	2300
1.1-3.1	4.5	2.54	2900
3.1-7.8	6.22	3.52	3100
>7.8	6.75	3.8	3300

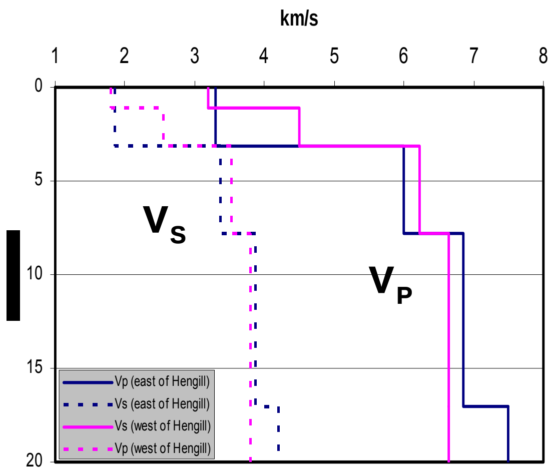

Dynamic stresses at the two hypocenters

- Nord - Sud vertical right - lateral faults
- $\Delta CFF = \Delta\tau + \mu(1 - B)\Delta\sigma_n$, with $\mu = 0.75$, $B = 0.47$
- Rise time: 1.6 s

26 s aftershock

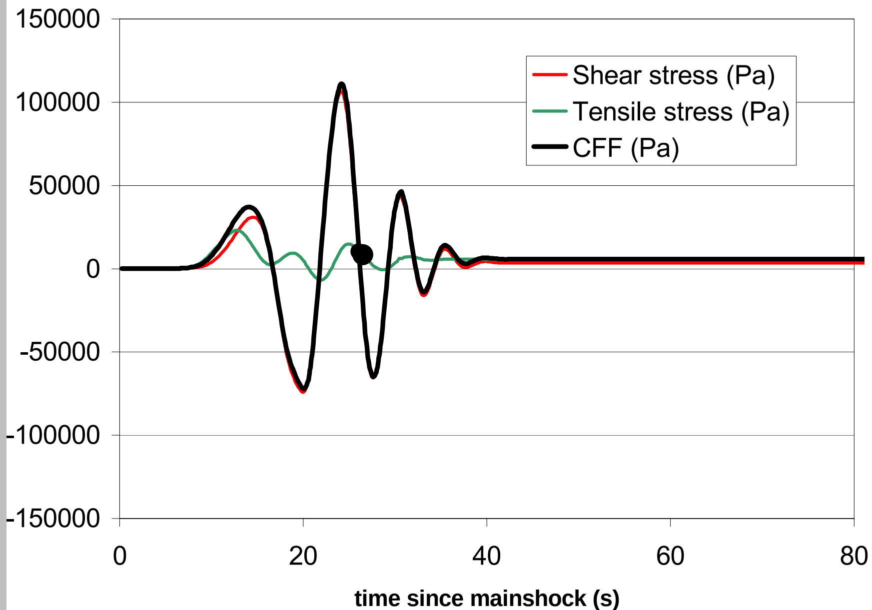

30 s aftershock

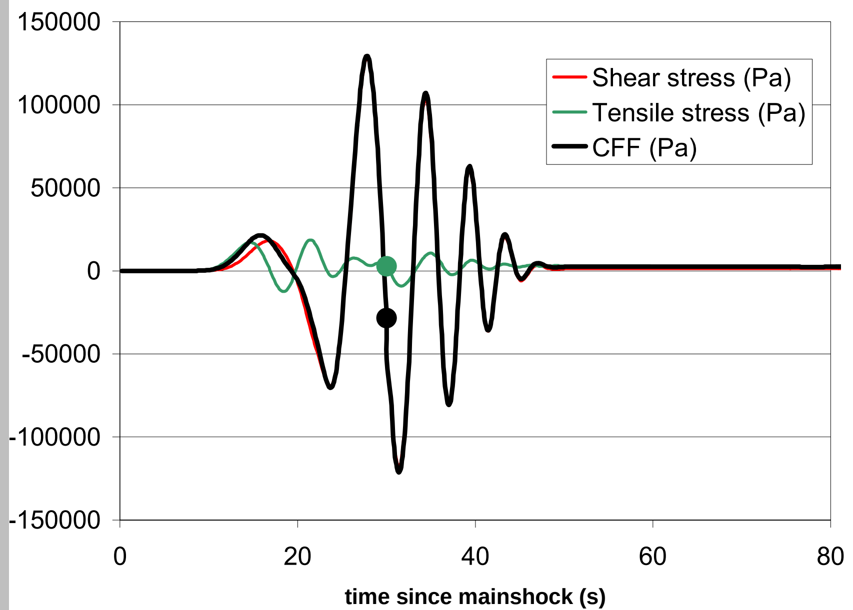

$\Delta CFF(t)$ at the two hypocenters

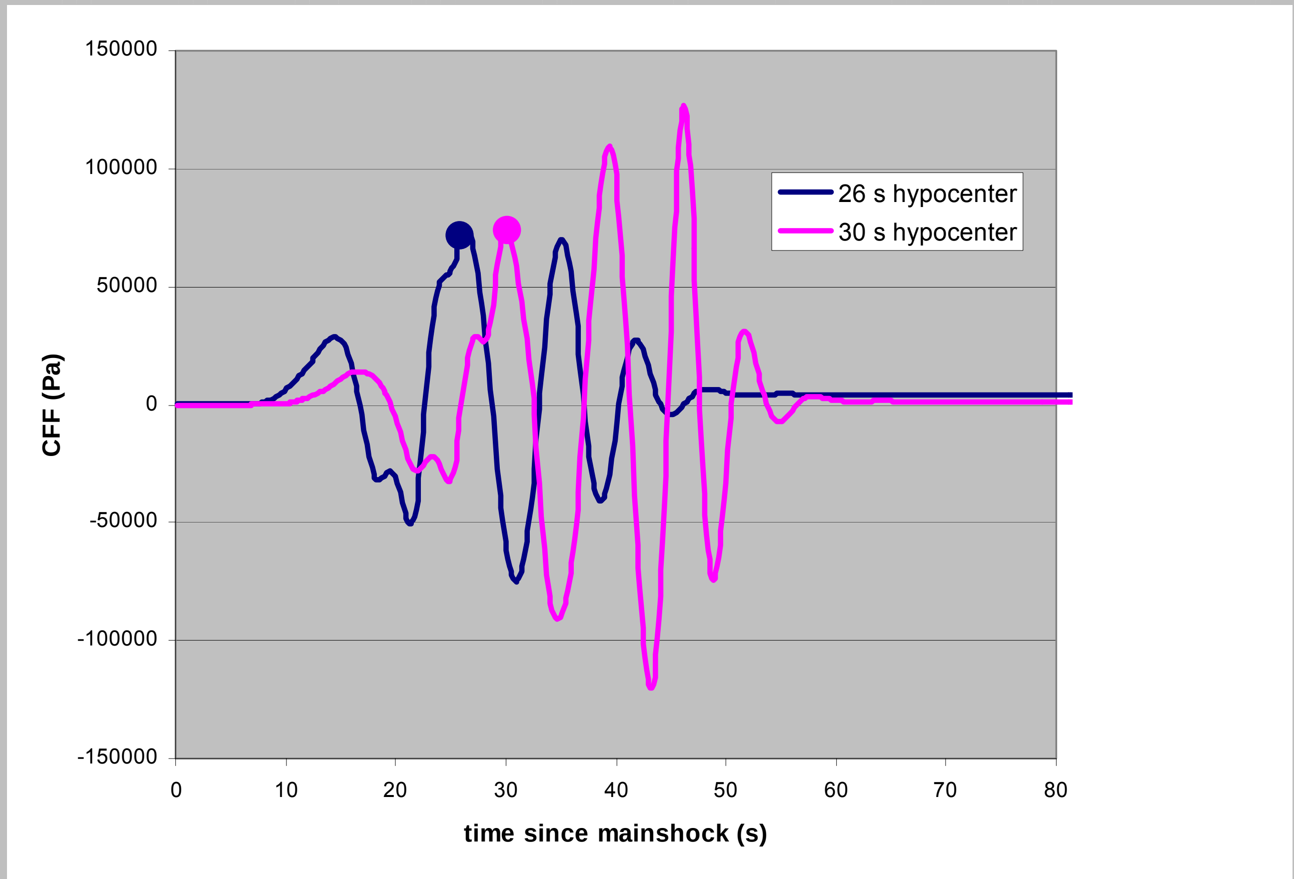

Time separation between the events and between stress peaks comparable.

Snapshots of dynamic stress

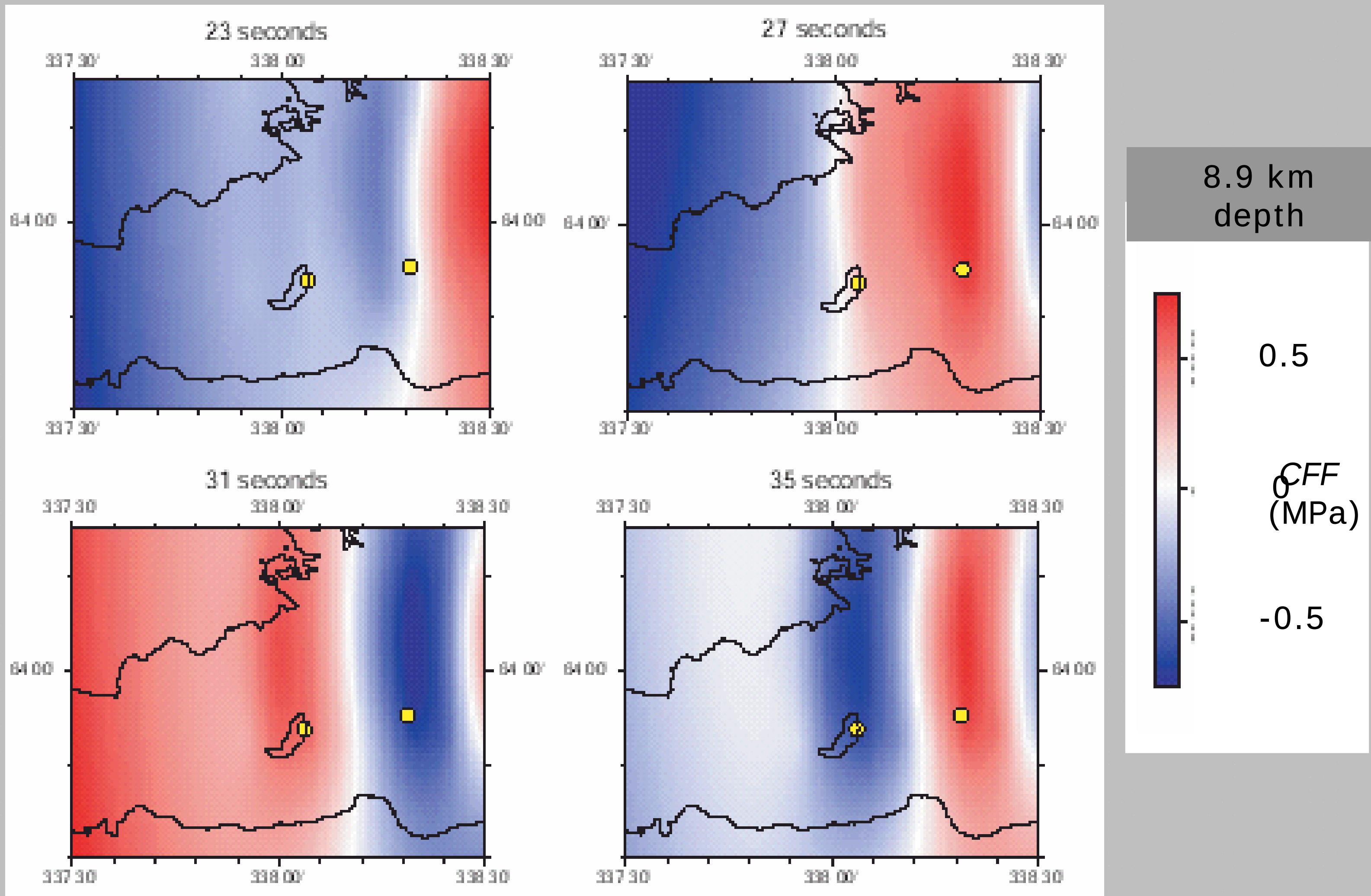

Parameters sensitivity #1

- Stress at each hypocenter is affected by uncertain parameters such as the crustal model, rise time and the hypocentral depth.
- **Crustal model**

26 s aftershock

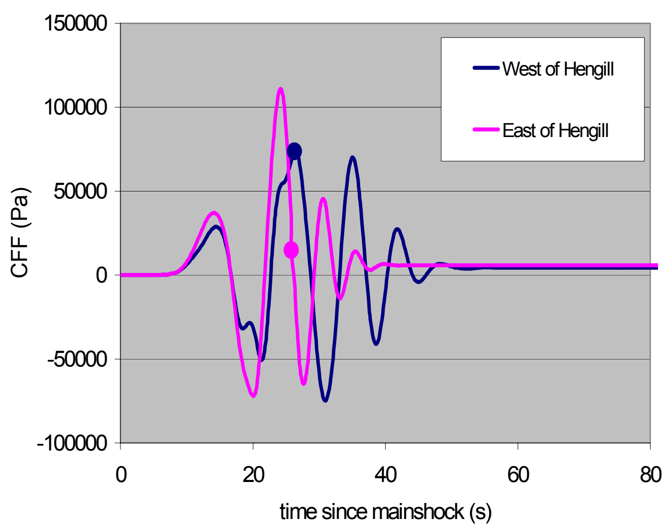

30 s aftershock

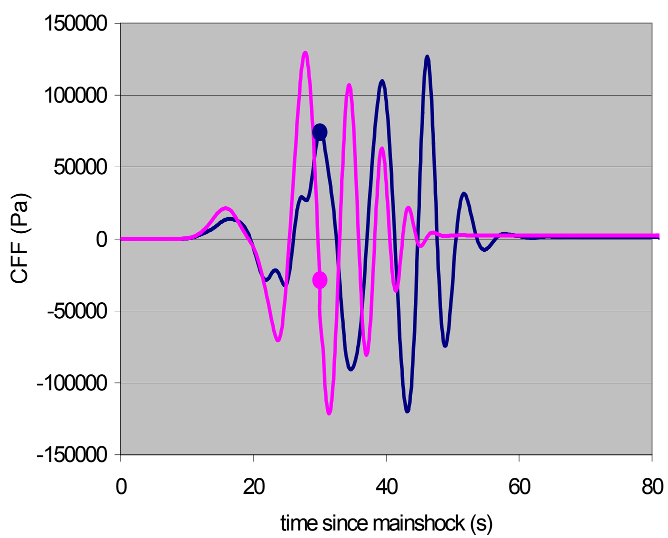

➢ The origin times (from mainshock) of the two events remain at, or follow closely the second CFF peak for ~ 1 - 2 s rise time.

Parameters sensitivity #2

Rise time

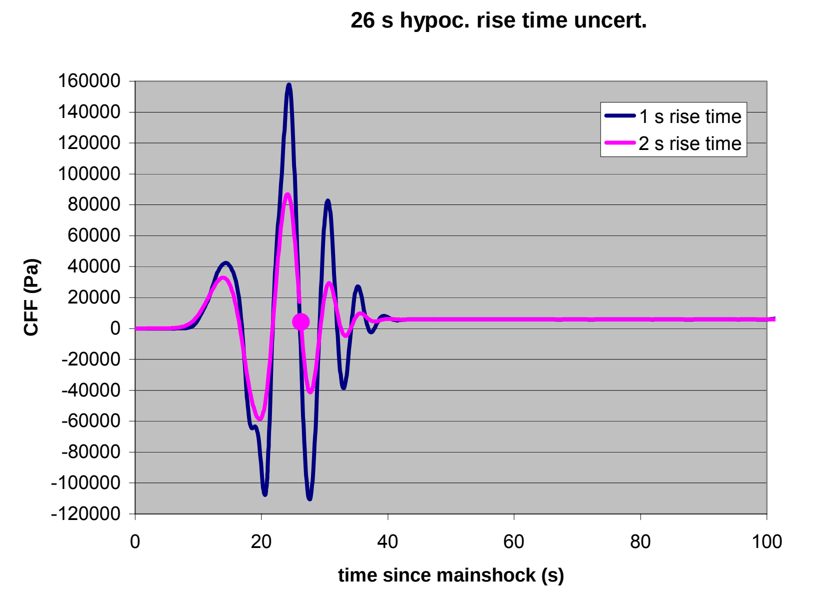

Hypocentral depth

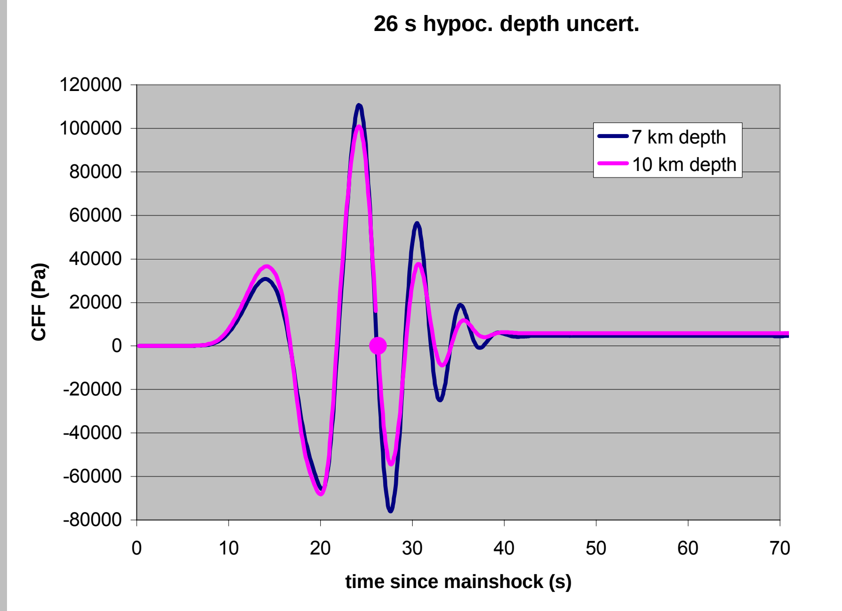

Uncertainties in stress amplitudes.

The fault response

- We study the fault response to the stress changes as evaluated at the two hypocenters with varying the parameters within their uncertaintes;
- We use a spring-slider model with rate- and state-dependent friction for variable effective normal stress σ_n^{eff};
- The system is perturbed either in shear stress and normal stress ($\Delta\tau(t)$, $\Delta\sigma_n^{eff}(t)$);
- We investigate the possibility of instantaneous triggering (during the transient stress perturbation).

Dieterich and Linker (1992)

$$\tau = \left[\mu_* + a\ln\left(\frac{v}{v_*}\right) + b\ln\left(\frac{\Psi v_*}{L}\right)\right]\sigma_n^{eff}(t)$$

$$\frac{\mathrm{d}}{\mathrm{dt}}\Psi = 1 - \frac{\Psi v}{L} - \alpha_{LD}\frac{\Psi\dot{\sigma}_n^{eff}}{b}$$

$$\alpha_{LD} = 0 \;\Rightarrow\; \sigma_n^{eff} = \sigma_n^{eff}(0)$$

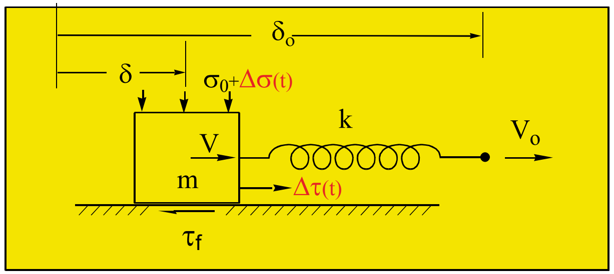

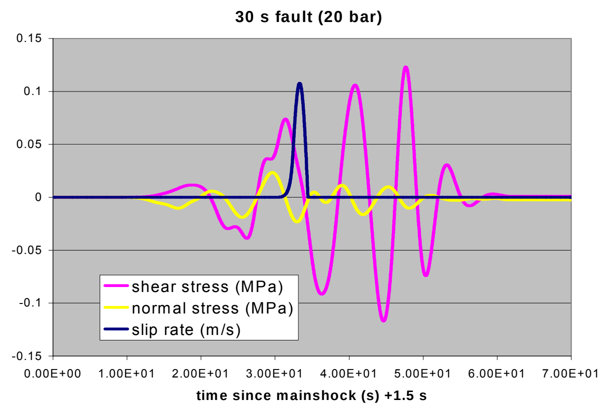

The instantaneous trigger

- h ~ 10 km linear fault dimension,
- standard values of rheological parameters ($\mu_* = 0.7$, $L = 1$ mm, $b = 0.01$),
- $v_0 = 2$ cm/yr (spreading rate in the SISZ),
- fault in close to failure conditions (100% steady state ❾ unperturbed failure expected at less than 2 yr from June 17, 2000)

➢ The fault tends to fail within 1 s after a peak in CFF, as evaluated at the two hypocenters

if

1. the initial effective normal stress σ_0 is enough low, so that the shear stress perturbation $\Delta\tau$ at that peak is much larger than $a(\sigma_0 + \Delta\sigma)$

2. and the direct effect of friction a is enough low to keep fault unstable ($k/k_{crit} < 1$) for low values of σ_0.

1-D Failure times of the perturbed faults

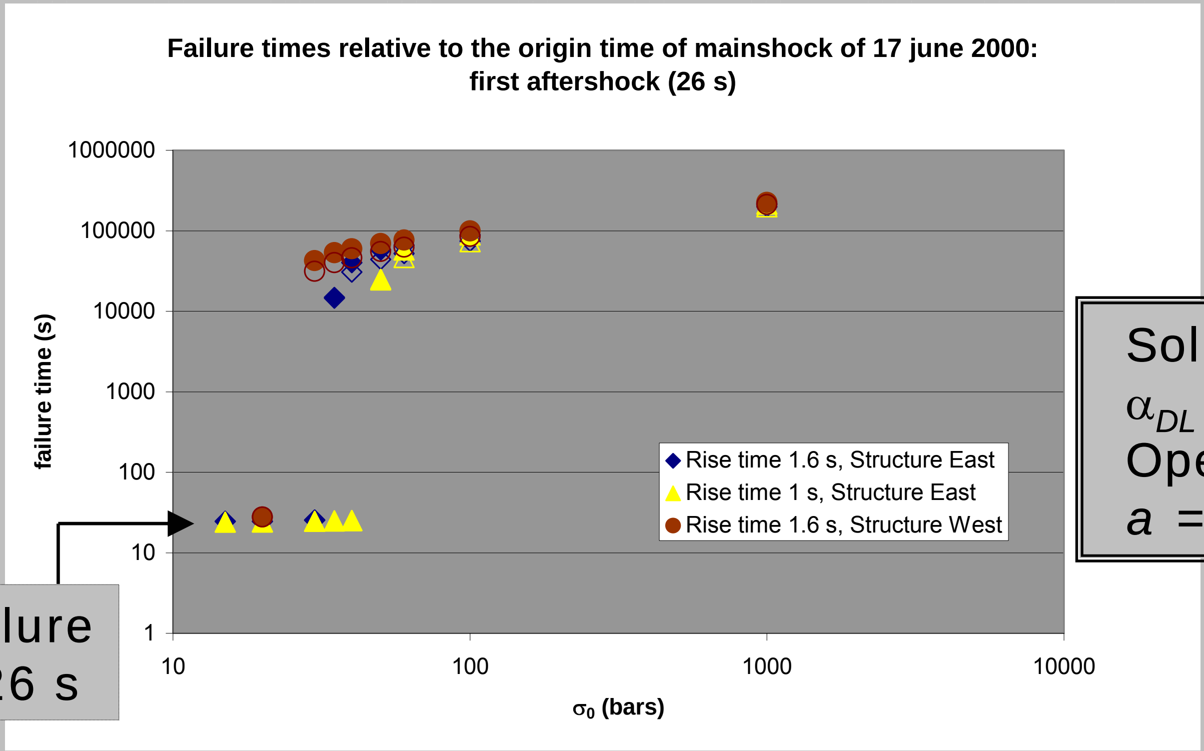

Mean failure time ≅ 26 s

Solid α_{DL}=0.56
Open α_{DL}=0
a = 0.003

- For $a \leq 0.003$ and $\sigma_0 \cong 20$ bar, we obtained instantaneous trigger within 1 second after the second peak of CFF, as expected for the two aftershocks in the SISZ.
- For $a = 0.003$ and $\sigma_0 > \gamma$ 20 bar, $1 < \gamma < 10$ (increasing with the amplitude of the second peak of $\Delta\tau$) the trigger is not instantaneous (failure time > 4 hours).

Conclusions I

- ✓ The 26 and 30 s events occurred near one of the important geothermal areas of Iceland;
- ✓ They were neglibly affected by static stress changes;
- ✓ They followed closely a peak of positive CFF;
- ✓ These results favour the hypothesis of dynamic triggering;
- ✓ Dynamic models of fault responses can explain observations for low values of effective normal stress (near lithostatic pore pressure).

Fault interaction by dynamic stress transfer: the case of the 2000 South Iceland seismic sequence

Part II

The va … up to
2.78 H … spaced
1650 m … 950 m,
6550 m

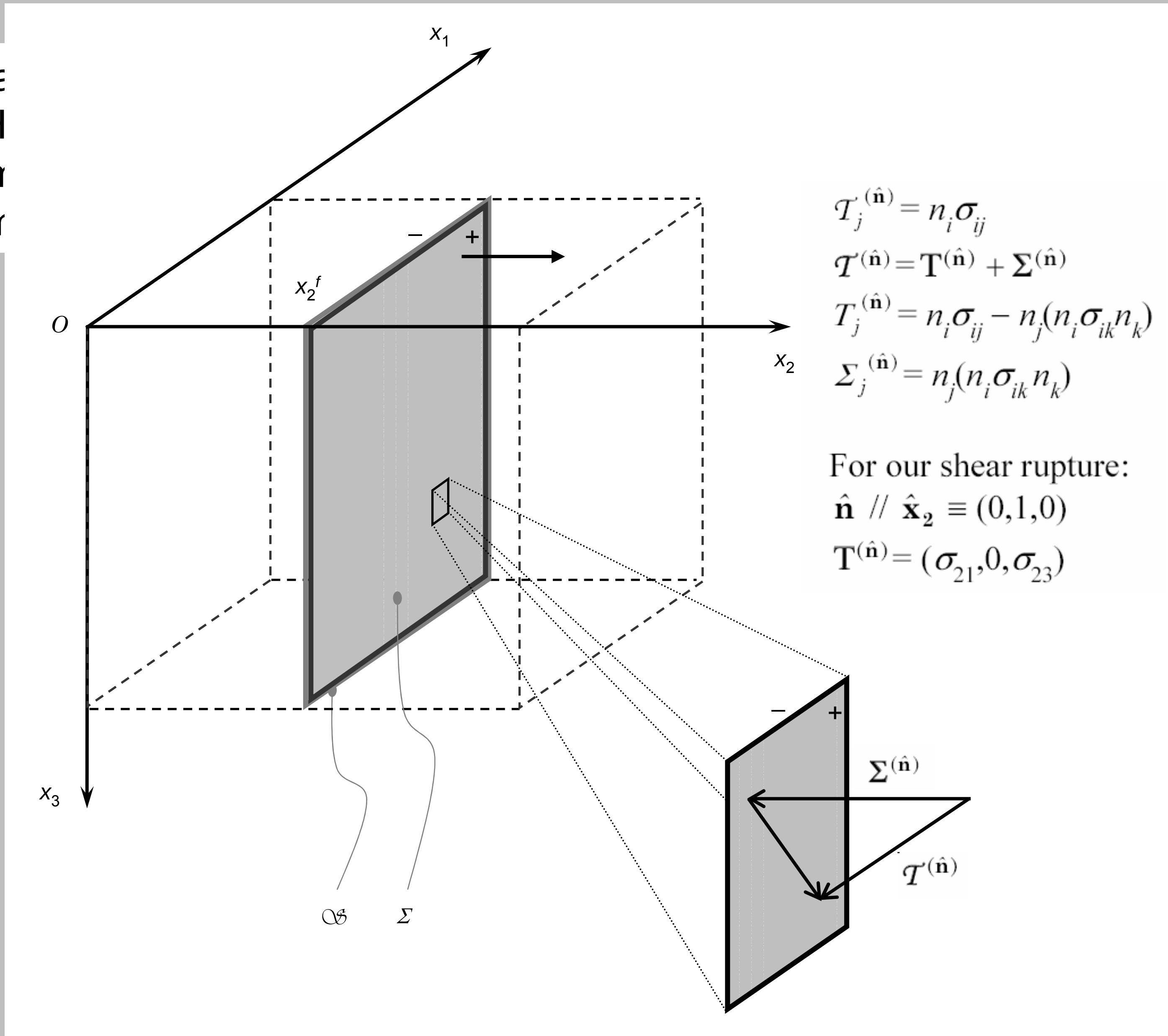

The spatial sampling of the receiver grid is not sufficient to correctly resolve the dynamic processes occurring during the rupture nucleation and propagation (Bizzarri and Cocco, 2003; 2005), as well as the temporal discretization.

We develop an algorithm that employs a $\mathcal{C}^2$ cubic spline to interpolate $\Delta\sigma_{ij}$ in space and in time.

Original values (*t* = 26.37 s)

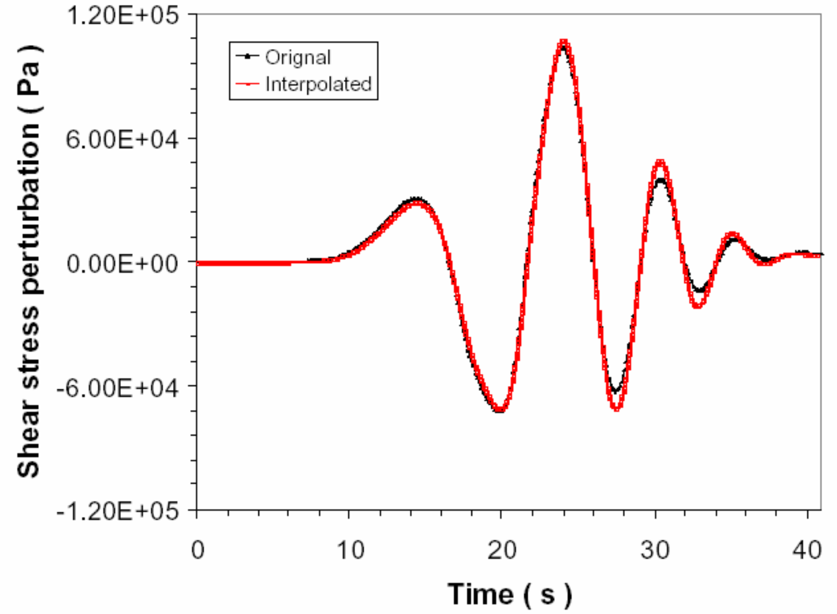

Interpolated values (*t* = 26.37 s)

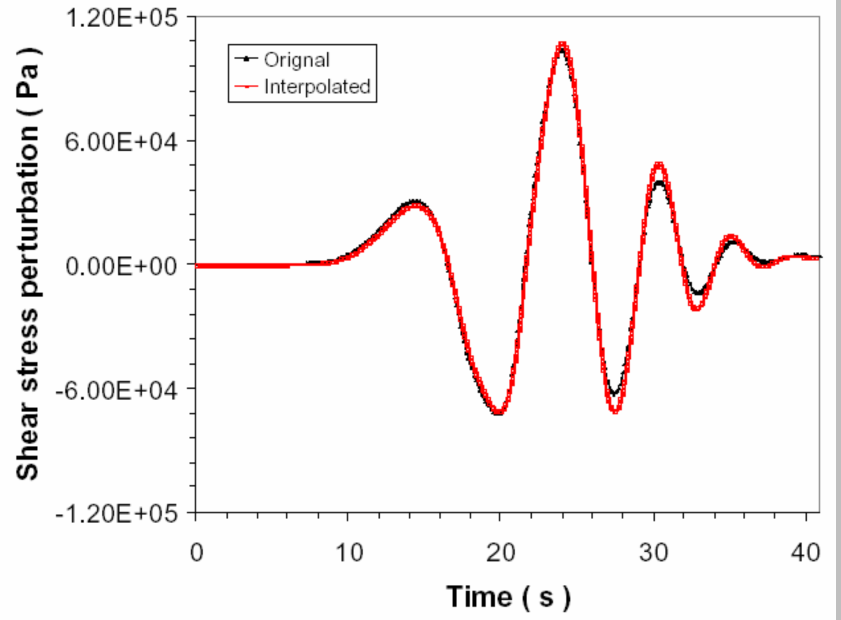

At time t, in each fault node, the dynamic load is: $\mathcal{L}_i = f_{ri} + T_{0i} + \Delta\sigma_{2i}$ (i = 1 and 3).

T_{0i} are the components of the initial traction ($\mathrm{T}_{\mathbf{0}}(x_1, x_3) = \tau_0(x_1, x_3)(\cos(\varphi_0), 0, \sin(\varphi_0))$)

f_{ri} are the components of the load (namely the contribution of the restoring forces, $\mathbf{f}_{\mathbf{r}}$) exerted by the neighboring points:

$$f_{ri} = (M^- f_i^+ - M^+ f_i^-)/(M^+ + M^-),$$

where M^+ and M^- are the masses of the "+" and "–" half split–node of the fault plane Σ and $\mathbf{f}^+$ is the force acting on partial node "+" caused by deformation of neighbouring elements located in the "–" side of S (and viceversa for $\mathbf{f}^-$).

$\{\Delta\sigma_{2i}\}$ are coupled to the components of the fault friction T_i via

$$\frac{\mathrm{d}^2}{\mathrm{d}t^2} u_1 = \alpha[\mathcal{L}_1 - T_1]$$
$$\frac{\mathrm{d}^2}{\mathrm{d}t^2} u_3 = \alpha[\mathcal{L}_3 - T_3]$$

where $\alpha \equiv \mathcal{A}\ ((1/M^+) + (1/M^-))$, $\mathcal{A} = \Delta x_1 \Delta x_3$. T_i express on the governing law.

Observational constraints

1) Perturbed rupture time $t_r = 25.9 \pm 0.1$ s

2) Hypocenter (63.951 ± 0.004 °N, 21.689 ± 0.008 °W, 8.9 ± 1.3 Km) ↔ on fault coordinates of (16500 ± 450, 8900 ± 1300) m (Antonioli et al., 2005)

3) From the aftershocks distribution shown in Hjaltadottir and Vogfjord (2005) we consider the seismic part of the fault (A) limited in latitude between 63.890 °N and 63.951 °N (in the case of Nord–South fault this corresponds to [9700, 16500] m in strike direction) and limited in depth between 5400 m and 7400 m

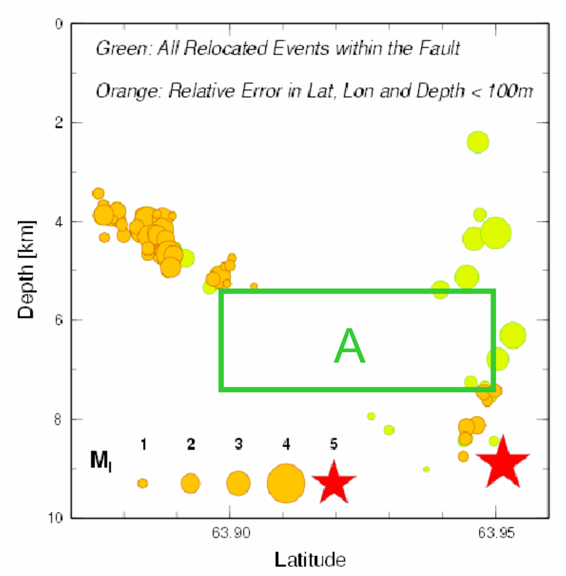

Upper bound estimates:

$M_0 = 1.23 \times 10^{15} A^{3/2} = 6.15 \times 10^{16}$ Nm;

Av. fault slip: $\langle u \rangle_A = M_0/(\rho v_S^2 A) = 0.12$ m;

Av. stress drop: $\langle \Delta\tau \rangle_A = 2M_0/(\pi W_A L_A) = 1.44$ MPa

4) $M_w \geq 5$ (Arnadottir et al., 2006; Vogfiord, 2003) $\Rightarrow M_0 \cong 3.2 \times 10^{16}$ Nm

Results with DR law – homogeneous

Dieterich – Ruina governing law

$$\tau = \mu(v,\Psi)\sigma_n^{eff} = \left[\mu_* + a \ln\left(\frac{v}{v_*}\right) + b \ln\left(\frac{\Psi v_*}{L}\right) \right] \sigma_n^{eff}$$

$$\frac{d}{dt}\Psi = 1 - \frac{\Psi v}{L}$$

Can be neglected (see Antonioli et al., 2005)

Perturbed rupture times

$v(x_1,x_3,t) \geq v_l \quad \Rightarrow \quad t_p(x_1,x_3) = t$

v_l = 0.1 m/s, in agreement with Belardinelli at al. (2003); Antonioli et al. (2005); Rubin and Ampuero (2005); Ziv and Cochard (2006)

σ_n^{eff} = 2.5 MPa everywhere; acting only $\Delta\sigma_{21}$

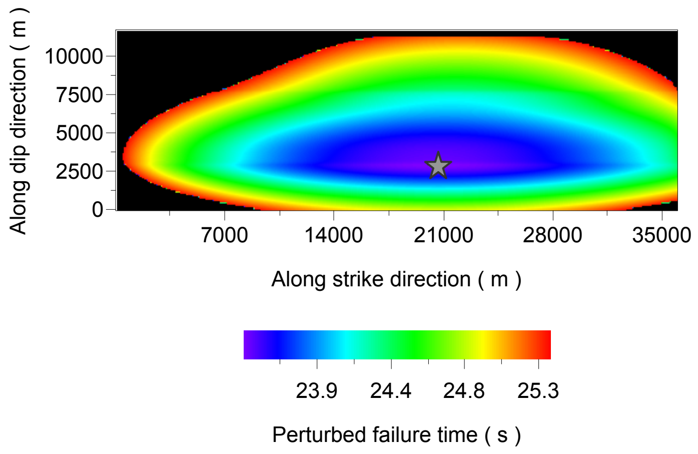

t_p^{min} = 23.47 s @ (20700,2900) m

M_0 = 2.37 x 10^{19} Nm

Whole fault

From Bizzarri and Belardinelli (Nov. 2005; subm. to JGR)

Results with DR law – homogeneous

Dieterich – Ruina governing law

$$\tau = \mu(v,\Psi)\sigma_n^{eff} = \left[\mu_* + a\ \ln\left(\frac{v}{v_*}\right) + b\ \ln\left(\frac{\Psi\ v_*}{L}\right)\right]\sigma_n^{eff}$$

$$\frac{d}{dt}\Psi = 1 - \frac{\Psi\ v}{L}$$

Can be neglected (see Antonioli et al., 2005)

Perturbed rupture times

$v(x_1,x_3,t) \geq v_l \quad \Rightarrow \quad t_p(x_1,x_3) = t$

v_l = 0.1 m/s, in agreement with Belardinelli at al. (2003); Antonioli et al. (2005); Rubin and Ampuero (2005); Ziv and Cochard (2006)

σ_n^{eff} = 2.5 MPa everywhere; acting also $\Delta\sigma_{22}$

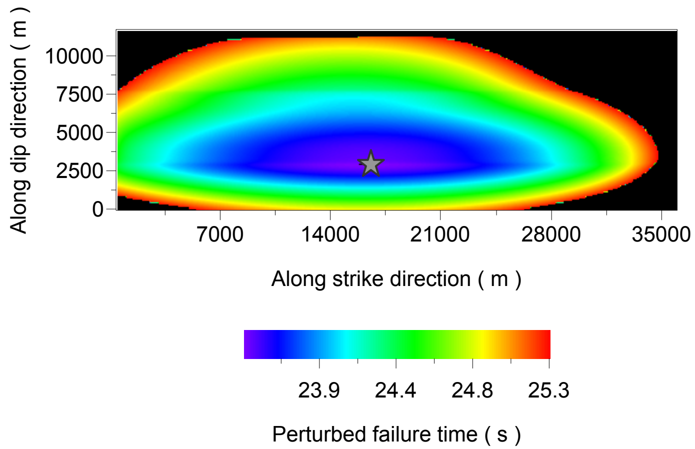

t_p^{min} = 23.47 s @ (16500,2900) m

M_0 = 2.23 x 10^{19} Nm

Whole fault

From Bizzarri and Belardinelli (Nov. 2005; subm. to JGR)

3-D Results with DR law – heterogeneous

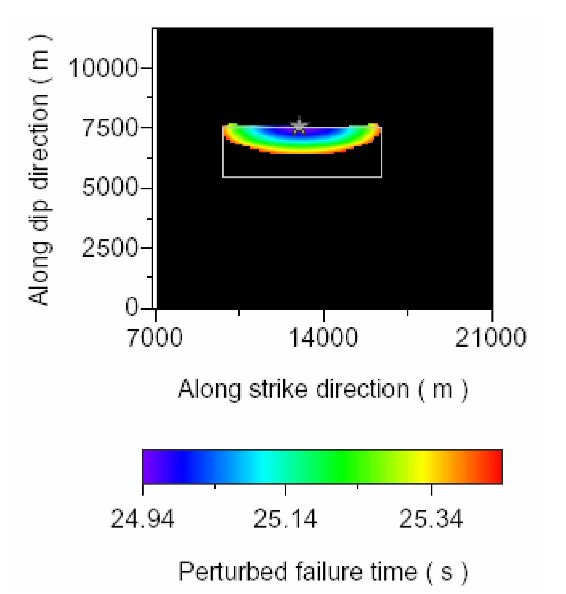

Velocity strengthening behavior ($a > b$) for $x_1 < 9700$ m, $x_1 > 16500$ m, $x_3 > 8800$ m

Effective normal stress profile

$t_p^{min} = 24.94$ s @ (13200,7500) m

$M_0 = 2.27 \times 10^{16}$ Nm

[9700,16500] m in strike direction

[6400,7500] m in dip direction

From Bizzarri and Belardinelli (Nov. 2005; subm. to JGR)

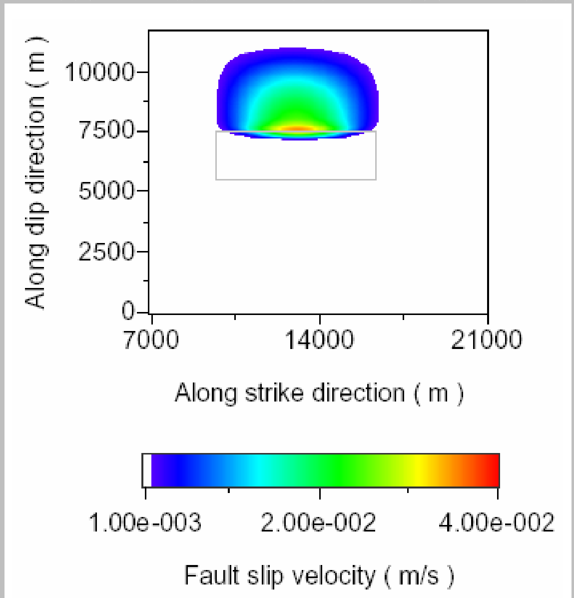

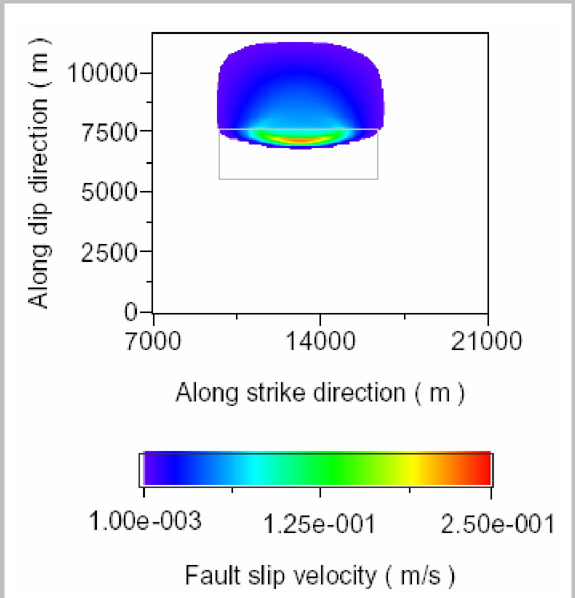

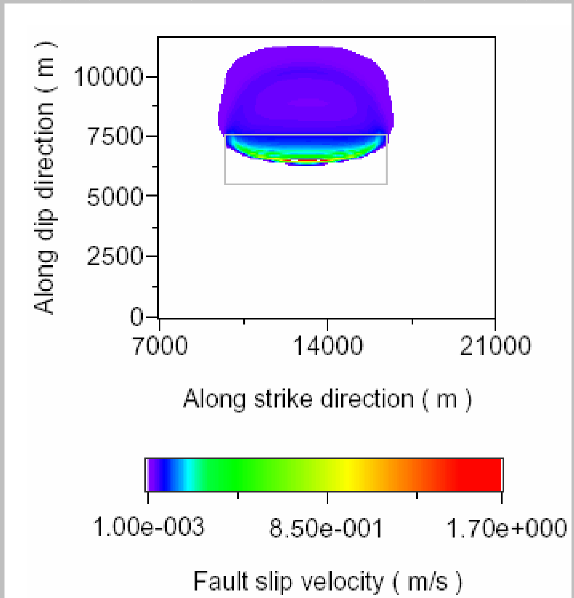

3-D

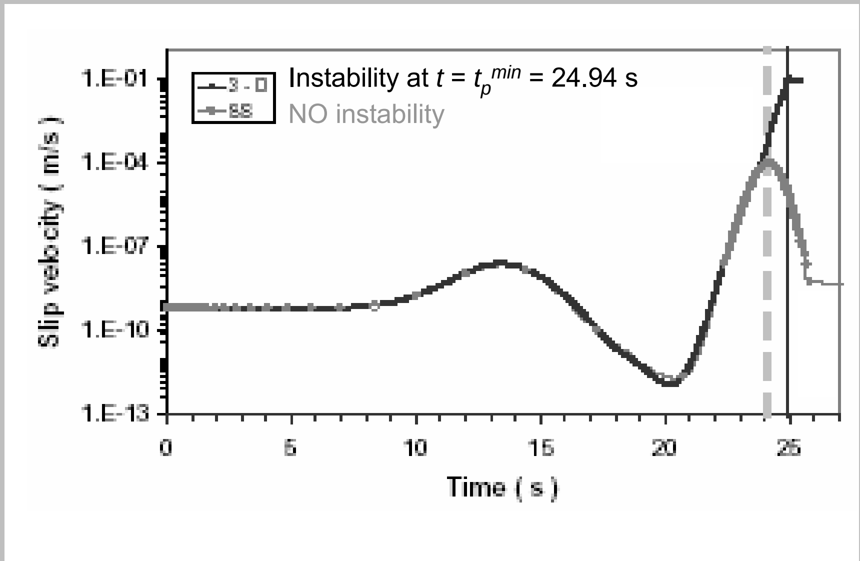

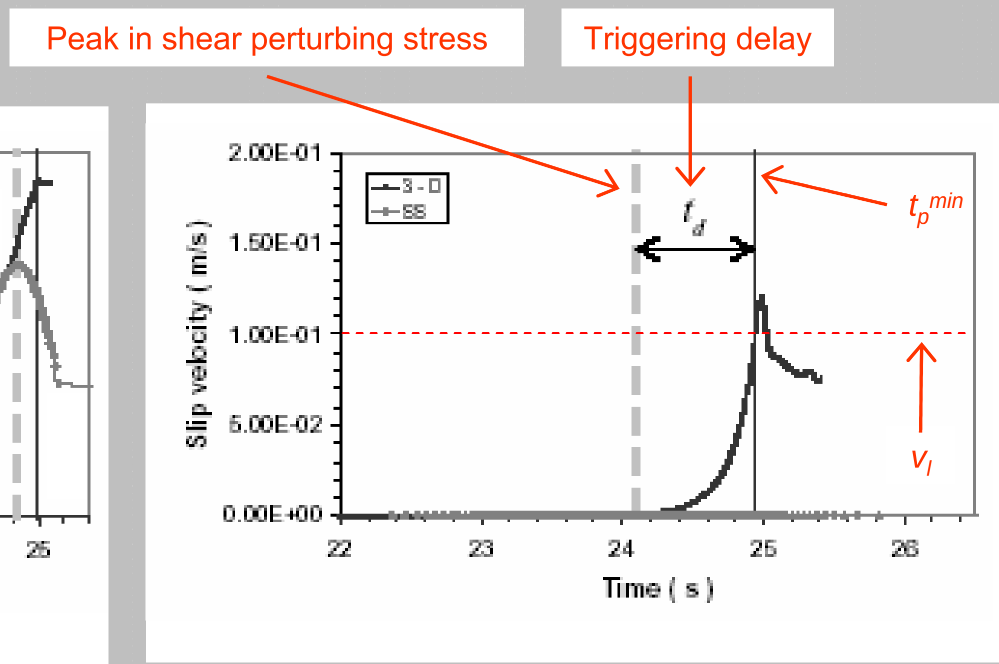

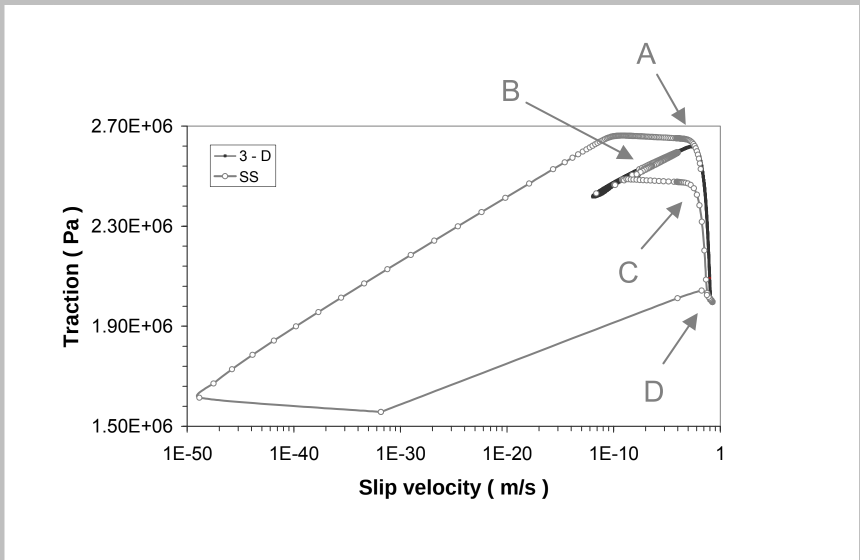

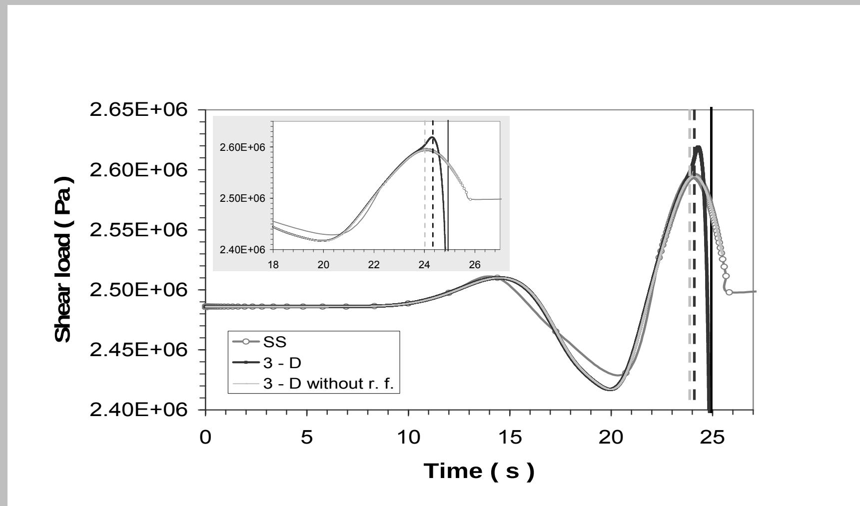

From Bizzarri and Belardinelli (Nov. 2005; subm. to JGR)

Results with RD law – heterogeneous

Ruina – Dieterich governing law

$$\tau = \left[\mu_* + a\ln\left(\frac{v}{v_*}\right) + b\ln\left(\frac{\Psi v_*}{L}\right)\right]\sigma_n^{eff}$$

$$\frac{d}{dt}\Psi = -\frac{\Psi v}{L}\ln\left(\frac{\Psi v}{L}\right)$$

Can be neglected

t_p^{min} = 23.44 s @ (15700,7900) m

M_0 = 2.02 x 10^{16} Nm

[9000,17300] m in strike direction

[6300,8000] m in dip direction

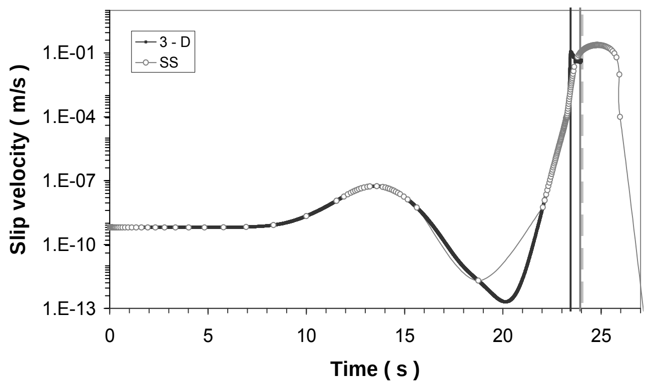

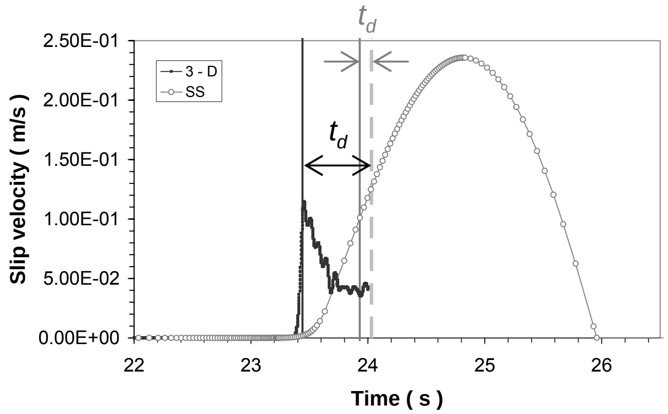

From Bizzarri and Belardinelli (Nov. 2005; subm. to JGR)

In the “virtual” hypocenter

Dieterich – Ruina governing law

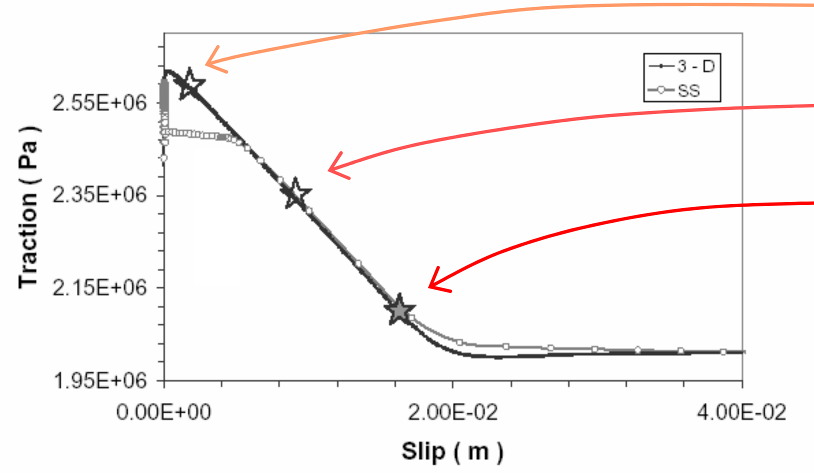

v^H = 0.01 m/s (t = 24.56 s)

v^H = 0.05 m/s (t = 24.84 s)

$v^H = v_l$ = 0.1 m/s ($t = t_p$ = 24.94 s)

Failure occurs before traction reaches the residual level.

Ruina – Dieterich governing law

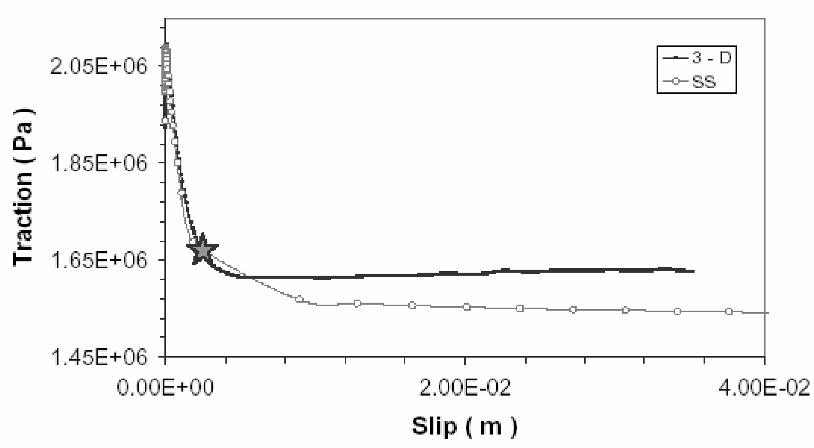

RD with L = 5 mm:

t_p^{min} = 23.99 s @ (14600,7600) m

$M_0 = 1.27 \times 10^{16}$ Nm

[9500,16800] m in strike direction

[6500,7700] m in dip direction

RD with L = 10 mm

t_p^{min} = 24.72 s @ (13300,7300) m

$M_0 = 2.27 \times 10^{16}$ Nm

[9500,16700] m in strike direction

[6000,7400] m in dip direction

From Bizzarri and Belardinelli (Nov. 2005; subm. to JGR)

Alternative source time functions

Bouchon source time function:

$$f(t)=\frac{1}{2}\left[1+\tanh\left(\frac{t}{t_0}\right)\right]$$

Bouchon, 1981; t_0 = 1.6 s

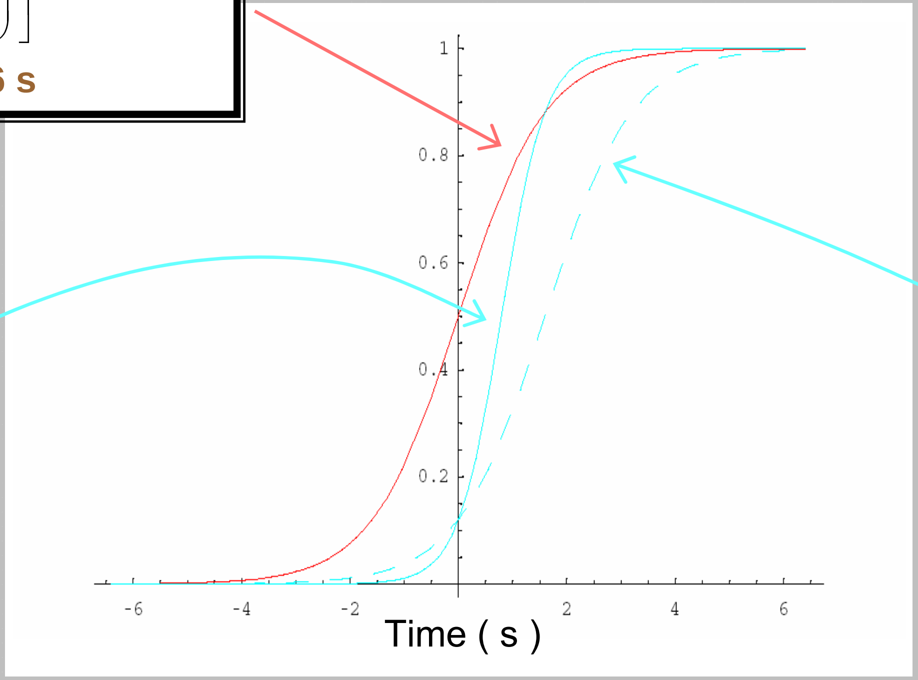

Modified Bouchon source time function:

$$f(t)=\frac{1}{2}\left[1+\tanh\left(\frac{t-\frac{t_0}{2}}{\frac{t_0}{2}}\right)\right]$$

corrected from Cotton and Campillo, 1995; t_0 = 1.6 s

Modified Bouchon source time function:

$$f(t)=\frac{1}{2}\left[1+\tanh\left(\frac{t-\frac{t_0}{2}}{\frac{t_0}{2}}\right)\right]$$

corrected from Cotton and Campillo, 1995; t_0 = 3.2 s

Alternative source time functions

Bouchon modificata, t_0 = 3.2 s

t_p^{min} = 26.49 s @ (13000,7500) m

$M_0 = 2.30 \times 10^{16}$ Nm

[9700,16500] m in strike direction

[6400,7600] m in dip direction

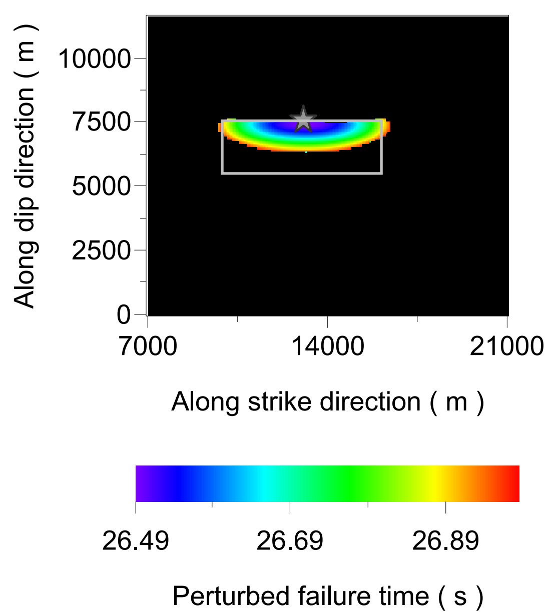

Bouchon modificata, t_0 = 1.6 s; σ_n^{eff*} = 4.2 MPa

t_p^{min} = 25.36 s @ (13500,7600) m

$M_0 = 2.59 \times 10^{16}$ Nm

[9500,16700] m in strike direction

[6200,8700] m in dip direction

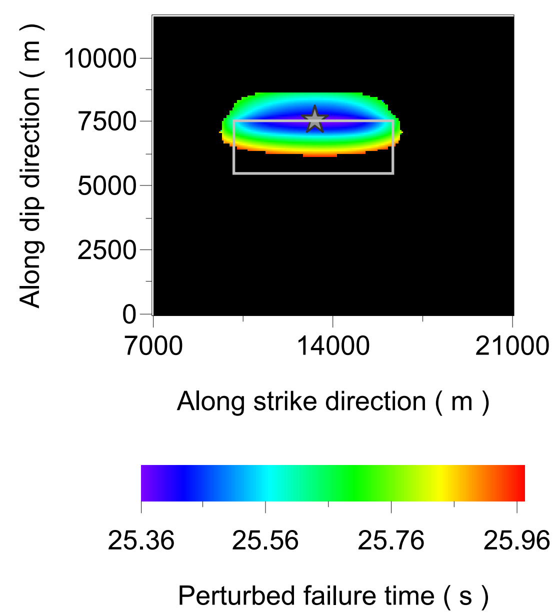

From Bizzarri and Belardinelli (Nov. 2005; subm. to JGR)

Conclusions II

- ✓ We simulate the remote triggering in a truly 3–D fault model with different governing laws;
- ✓ We generalize the results of Antonioli et al. (2006), providing additional details of the 26 s event: the location of the hypocenter, its failure time, the rupture area and the seismic moment;
- ✓ The spring–slider and the 3–D model are intrinsically different, but we observe an excellent agreement during the slow nucleation phase…
- ✓ … during the acceleration, in the 3–D model the dynamic load of the slipping points further decrease the perturbed failure time;
- ✓ Dieterich–Ruina and Ruina–Dieterich laws are valid candidate to model the activation of the Hvalhnúkur fault at 26 s;

- ✓ On the contrary, with slip–dependent friction laws it is not possible to simulate the activation of the 26 s aftershock;
- ✓ The agreement with observations increases considering a modified (and more causal) source time function;
- ✓ If a detailed information of the initial state of the fault, potentially highly heterogeneous, was available the agreement with observations will be even better.

Synopsis

Case	σ_{n0}^{eff} *profile*	*Constitutive law*	*Heterogeneous rheology*	*Rupture extension along strike* (m)	*Rupture extension along dip* (m)	*Hypocenter location* (m)	*Origin time* (s)	*Total seismic moment* M_0 (Nm)
A	(b)	DR	No	Whole fault	Whole fault	(20700,2900)	23.47	2.37×10^{19}
B	(b)	DR	No	Whole fault	Whole fault	(16500,2900)	23.47	2.23×10^{19}
C	1	DR	No	[0, 27400]	[6000, 11600]	(15400,6600)	24.08	1.94×10^{17}
D	2	DR	No	Not defined				1.21×10^{14}
E	3	DR	No	[6600, 20000]	[6400, 7500]	(13200,7500)	24.94	6.43×10^{16}
F	3	DR	Yes	[9700, 16500]	[6400, 7500]	(13200,7500)	24.94	2.27×10^{16}
G	3	DR	No	[15700, 35100]	[6000, 7800]	(27300,7500)	23.44	1.22×10^{17}
H	3	RD	Yes	[9000, 17300]	[6300, 8000]	(15700,7900)	23.44	2.02×10^{16}
I	3	RD (L = 5 mm)	Yes	[9500, 16800]	[6500, 7700]	(14600,7600)	23.99	1.27×10^{16}
L	3	RD (L = 10 mm)	Yes	[9500, 16700]	[6000, 7400]	(13300,7300)	24.72	2.17×10^{16}
M	3	OY	Yes	Not defined				1.46×10^{14}
N	3	OY	No	Whole fault	Whole fault	(24000,7700)	23.75	2.49×10^{19}
O	3	DR	Yes	[9700, 16500]	[6400, 7600]	(13000,7500)	26.49	2.30×10^{16}
P	3	DR	Yes	[9500, 16700]	[6200, 8700]	(13500,7600)	25.36	2.59×10^{16}
Observational constraints				**[9700, 16500]**	**[5400, 7400]**	**(16500 ± 450, 8900 ± 1300)**	**25.9 ± 0.1**	$\cong$ **3.2** $\times 10^{16}$

This slide is empty intentionally.

A B R

Support Slides:
Parameters, Notes, etc.

To not be displayed directly. Referenced above.

Geothermal areas in Iceland

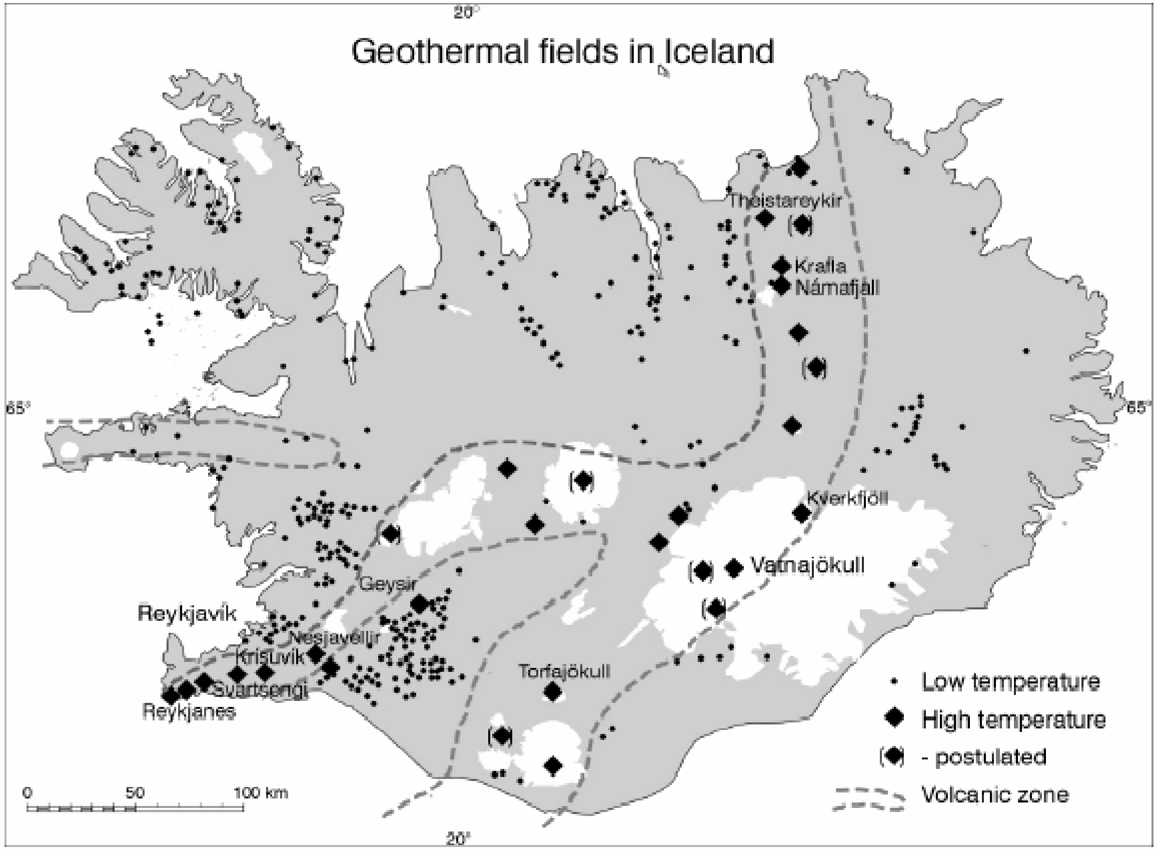

Proceedings World Geothermal Congress 2000
Kyushu - Tohoku, Japan, May 28 - June 10, 2000

NATURAL CHANGES IN UNEXPLOITED HIGH-TEMPERATURE GEOTHERMAL AREAS IN ICELAND

Halldór Ármannsson[1], Hrefna Kristmannsdóttir[1], Helgi Torfason[2] and Magnús Ólafsson[1]
Orkustofnun, [1]Research Division, Geochemistry Department, [2]Energy Management Division
Grensásvegur 9, 108 Reykjavík

Figure 1. Geothermal areas in Iceland. The five main exploited high-temperature areas, Svartsengi, Reykjanes, Nesjavellir, Krafla and Námafjall are shown as well as the four unexploited high-temperature geothermal areas selected for study of natural changes, Krýsuvík, Theistareykir, Torfajökull and Kverkfjöll areas.

Parameter	***Value***
$\mathcal{D}$	parallelepiped that extends $x_{1_{end}} = 36.5$ Km along x_1, $x_{2_{end}} = 10$ Km along x_2 and $x_{3_{end}} = 11.6$ Km along x_3
$\Sigma = \mathcal{S}$	$\{ \mathbf{x} \mid x_2 = x_2^f = 5000 \text{ m} \}$
$\Delta x_1 = \Delta x_2 = \Delta x_3 \equiv \Delta x$	100 m (a)
Number of nodes	4,289,571
Δt	1.27×10^{-3} s (a)
Number of time levels	33,650
v_l	0.1 m/s
$\sigma_n^{eff^*}$	2.5 MPa
$\varphi(x_1, x_3, 0)$	$\varphi_0 = 180°$
$v(x_1, x_3, 0)$	$v_{init} = 6.34 \times 10^{-10}$ m/s (= 20 mm/yr)
$\Psi(x_1, x_3, 0)$	$\Psi^{ss}(v_{init}) = 1.577 \times 10^6$ s ($\cong$ 18.25 d)
$\sigma_n^{eff}(x_1, x_3, 0)$	See Table 3
$\tau_0(x_1, x_3)$	$\mu^{ss}(v_{init})\sigma_n^{eff}(x_1, x_3, 0)$
a	0.003 (b)
b	0.010
L	1×10^{-3} m
μ_*	0.7
v_*	v_{init}
α_{LD}	0

Crustal profile (from Vogfjord et al., 2002; Antonioli et al., 2005)

***Layer* # k**	v_{P_k} (m/s)	v_{S_k} (m/s)	ρ_{rock_k} (Kg/m^3)	***Up do depth of* x_{3_k} (m)**
1	3200	1810	2300	1100
2	4500	2540	2540	3100
3	6220	3520	3050	7800
4	6750	3800	3100	11600

Initial effective normal stress

$$\sigma_{n_0}^{eff}(x_3) \equiv \sigma_n^{eff}(x_1,x_3,t) =$$

$$\begin{cases} \hat{p}^{(litho)}(x_3) - \Delta\sigma^{(dev)} - p_{fluid}^{(hydro)}(x_3) & , x_3 \le x_3^* = 5800\text{ m} \\ \hat{p}^{(litho)}(x_3) - \Delta\sigma^{(dev)} - \left[\hat{p}^{(litho)}(x_3) - \Delta\sigma^{(dev)} - \sigma_n^{eff^*} - \Delta P_2\, e^{-\frac{x_3 - x_3^*}{h^*}} + \sigma_n^{eff^*} e^{-\frac{x_3 - x_3^*}{h^*}} \right] & , x_3^* < x_3 < x_3^* + D^* \\ \sigma_n^{eff^*} = 2.5\text{ MPa} & , x_3 \ge x_3^* + D^* = 8800\text{ m} \end{cases}$$

$$\Delta P_2 \equiv \hat{p}^{(litho)}(x_3^*) - \Delta\sigma^{(dev)} - p_{fluid}^{(hydro)}(x_3^*)$$